

DYSON-SCHWINGER-EQUATIONS IN MINIMAL SUBTRACTION

PAUL-HERMANN BALDUF

ABSTRACT. We examine selected one-scale Dyson-Schwinger-equations in the minimal subtraction renormalization scheme and dimensional regularization. They are constructed from three different integral kernels; two one-loop Feynman integrals and one toy model. For each of the kernels, we examine both linear and non-linear DSEs. We confirm that the solutions in minimal subtraction are equal to the ones in kinematic renormalization, but with a shifted renormalization point. We compute various series expansions symbolically to at least ten loop order and numerically to higher order. In the linear cases, we identify the so-obtained sequences and find an analytic generating function for the shift of the renormalization point. In the non-linear DSEs, the results for the shift suggest a factorially divergent power series. We determine the leading asymptotic growth parameters and find them in agreement with the ones of the anomalous dimension. Finally, we compute coefficients of the MS-counter terms Z and confirm, for the linear DSEs, a closed form expression consistent with the literature.

1. INTRODUCTION

1.1. Motivation. So far, the systematic Hopf-algebraic treatment [27, 26, 34, 7, 6, 5, 24] of Dyson-Schwinger-equations (DSEs) [22, 32] has relied on kinematic renormalization schemes, called MOM hereafter. The solution of a DSE is the renormalized Green function $G_{\mathcal{R}}(p^2)$. MOM schemes assign a value to the renormalized Green function $G_{\mathcal{R}}(p^2)$ at one particular momentum $p^2 = \mu^2$, and thereby have a transparent interpretation as boundary condition for the DSE. For a single (non-coupled) DSE, the only remaining unknown object is the anomalous dimension $\gamma_1(\alpha)$ as a function of the coupling α . If MOM-conditions are used systematically, explicit regularization of divergent integrals is not necessary [27, 26] and one only deals with finite quantities at all stages. In fact, $\gamma_1(\alpha)$ can be computed from a differential equation without any divergent integral. Even if the earlier works [20, 21] do regulate the integrals explicitly using dimensional regularization [2, 8], they still use MOM renormalization conditions.

On the other hand, many perturbative computations in quantum field theory use the combination of dimensional regularization and minimal subtraction (MS) renormalization conditions. In this scheme, all singular terms in the regulator ϵ are subtracted, but the resulting amplitude does not respect any particular kinematic boundary condition. The MS scheme can only be implemented by explicitly regulating and renormalizing the integrals at every loop order in the DSE since it is unknown how to define it via a direct condition for the solution $G_{\mathcal{R}}(p^2)$.

At the same time, different renormalization schemes should not lead to different physical outcomes, therefore, there ought to be *some* particular momentum $\hat{\mu}$ such that minimal subtraction agrees with kinematic renormalization using that very reference momentum $\hat{\mu}$. Finding this correspondence is of practical relevance since the perturbative solution is typically only known to a few orders. In that case, the truncated MS-renormalized and MOM-renormalized results are truly different and valid only around their respective renormalization points [14]. Knowing the physical value of the MS-renormalization point is then crucial for the validity range of the truncated Green function.

The author thanks Dirk Kreimer for encouragement and several discussions, and Gerald Dunne for comments and suggestions on the draft.

1.2. Content. In the present paper, we analyse Dyson-Schwinger-Equations based on three different primitive integral kernels. The first one is the 4-dimensional bubble (=1-loop-multiedge) graph appearing e.g. in the fermion propagator in Yukawa theory. The second one is the same graph in 6 dimensions, contributing to the ϕ^3 -propagator, and the third is a mathematical toy model which has occasionally been used to study renormalization. In all three cases, we consider the recursive insertion of the Green function into only one place in the kernel graph. First, we insert the Green function itself, which amounts to a linear DSE known as the rainbow approximation. Second, we insert the Green function raised to a power $\in \{-4, \dots, +6\}$, producing non-linear DSEs. We compute series coefficients, symbolically and numerically, of the various relevant quantities both in MOM- and in MS-renormalization in dimensional regularization.

Section 2 is a recap of the central theoretical concepts used in this paper. In section 3, the algorithm for linear DSEs is developed for the case of the 4-dimensional bubble integral. Subsequently, this is applied to the $D = 6$ case in section 4 and to the toy model in section 5. Then, in section 6, the algorithm is extended to non-linear DSEs and used for the 4-dimensional model. The last sections 7 and 8 contain the results for the non-linear DSEs for the two remaining models, $D = 6$ and the toy model. Section 9 is a summary of the results obtained.

2. THEORETICAL BACKGROUND

2.1. Unrenormalized Dyson-Schwinger-Equation. We consider DSEs of the form

$$(2.1) \quad G(\alpha, x) = 1 + \alpha \int dy K(x, y) Q(G(\alpha, y)) G(\alpha, y)$$

where $G(x)$ is the unrenormalized Green function and $K(x, y)$ is an integral kernel, determined by a single primitive Feynman diagram. Since we restrict to dependence on one single external scale, $K(x, y)$ stems from a propagator-type diagram and $G(x)$ represents the 1PI 2-point-function of the theory. The variable $x = p^2/\mu^2$ is the external momentum scaled to some reference momentum μ . In the literature, propagator-type DSE is often written with a minus sign, $G = 1 - \alpha \int \dots$. We will use a plus for all DSEs considered in this work.

The invariant charge in our cases is a monomial of the Green function,

$$(2.2) \quad Q(G(\alpha, x)) = (G(\alpha, x))^s.$$

The derivative of the renormalized invariant charge with respect to logarithmic momentum at the renormalization point (in MOM renormalization) is the beta function of the theory. For an invariant charge of the form eq. (2.2), the beta function is $\beta(\alpha) = s\gamma_1(\alpha)$, where $\gamma_1(\alpha)$ is the anomalous dimension. Especially, the choice $s = 0$ or $Q(G) \equiv 1$ corresponds to a theory with vanishing beta function, the Dyson-Schwinger-Equation is then linear.

2.2. Renormalization. We will only consider DSEs of multiplicatively renormalizable theories. This means that it is possible to eliminate all divergences at order m by two counter terms $Z_G^{(m)}$ and $Z_\alpha^{(m)}$. They act as a rescaling of the Green function and the coupling constant according to

$$(2.3) \quad \alpha = Z_\alpha(\alpha_{\mathcal{R}}) \cdot \alpha_{\mathcal{R}}, \quad G_{\mathcal{R}}(\alpha_{\mathcal{R}}, x) = Z_G(\alpha_{\mathcal{R}}) \cdot G(Z_\alpha(\alpha_{\mathcal{R}})\alpha_{\mathcal{R}}, x).$$

These Z -factors are themselves functions of $\alpha_{\mathcal{R}}$ and of the regularization parameter ϵ .

The renormalization of the coupling constant is only necessary if the theory has a non-vanishing beta function or, equivalently, a running coupling. See [28] for a recent account. Eventually, Z_α is given by the renormalization of the invariant charge Q . In the present case where there is only one Green function $G(\alpha, x)$ which needs renormalization, the invariant charge eq. (2.2) implies that

$$(2.4) \quad Z_\alpha(\alpha_{\mathcal{R}}) = (Z_G(\alpha_{\mathcal{R}}))^s.$$

Explicit renormalization requires to regulate the divergent integrals first. In dimensional regularization [2, 8], the space-time dimension is changed by a non-integer contribution ϵ , we choose $D = 4 - 2\epsilon$ or $D = 6 - 2\epsilon$. The unrenormalized amplitude of a finite graph is then a Laurent series in the regularization parameter ϵ .

It is possible to first solve the unrenormalized DSE eq. (2.1) and then afterwards determine the Z -factor order by order. However, it is more transparent to compute the Z -factor directly within the iterative solution of the DSE. To this end, one inserts eq. (2.1) into eq. (2.3) and uses eqs. (2.2) and (2.4) to obtain

$$\begin{aligned} G_{\mathcal{R}}(\alpha_{\mathcal{R}}, x) &= Z_G \left(1 + Z_{\alpha} \alpha_{\mathcal{R}} \int dy K(x, y) (G(Z_{\alpha} \alpha_{\mathcal{R}}, y))^{s+1} \right) \\ (2.5) \qquad \qquad &= Z_G + \alpha_{\mathcal{R}} \int dy K(x, y) Q(G_{\mathcal{R}}(\alpha_{\mathcal{R}}, y)) G_{\mathcal{R}}(\alpha_{\mathcal{R}}, y). \end{aligned}$$

This equation can be solved iteratively by inserting the solution of order $(m-1)$, $G_{\mathcal{R}}^{(m-1)}(\alpha_{\mathcal{R}}, y)$, into the right hand side to obtain the order- m -solution $G_{\mathcal{R}}^{(m)}(\alpha_{\mathcal{R}}, x)$. We assume that no IR-divergences appear. The integrand is finite because it is a power of a renormalized Green function, therefore the integral is only superficially divergent. The so-obtained divergence is of order $\alpha_{\mathcal{R}}^m$ and can be absorbed by a suitable summand in $Z_G^{(m)}$, producing a finite $G_{\mathcal{R}}^{(m)}(\alpha_{\mathcal{R}}, x)$.

Effectively, $\alpha_{\mathcal{R}}$ is just a different name for the expansion variable in eq. (2.5) compared to eq. (2.1). In order to streamline notation, we will in the following use α for the renormalized coupling and understand that $G_{\mathcal{R}}(\alpha, x)$ is short for $G_{\mathcal{R}}(\alpha_{\mathcal{R}}, x)$. In dimensional regularization the renormalized coupling obtains a factor μ^ϵ to make it dimensionless, we absorb this factor as well. Finally, we set $Z := Z_G$ for the only counter term in eq. (2.5).

The counter term is not unique because it is possible to include, apart from the divergence, also finite summands. Fixing it uniquely requires a renormalization condition. In the minimal subtraction scheme, $\hat{Z}^{(m)}$ consists of only the pole terms of the integral at order m ,

$$(2.6) \qquad \hat{Z}^{(m)} = \hat{Z}^{(m-1)} - \hat{\mathcal{R}} \left[\alpha \int dy K(x, y) Q \left(G_{\mathcal{R}}^{(m-1)} \right) G_{\mathcal{R}}^{(m-1)} \right] \quad (\text{MS scheme}).$$

The operator $\hat{\mathcal{R}}$ extracts only the pole terms in ϵ in dimensional regularisation. The MS-bar renormalization scheme is a variant of MS where those finite terms which arise from a series expansion of $\frac{e^{\gamma_E}}{4\pi}$ are also subtracted. On the other hand, the MOM scheme is defined by the requirement

$$(2.7) \qquad G_{\mathcal{R}}(\alpha, x = 1) = 1 \quad (\text{MOM scheme}).$$

This is achieved order by order if one includes not only the pole term, but all finite parts of the amplitude into the counterterm $Z^{(m)} = Z^{(m-1)} - \mathcal{R}[\dots]$. The MOM-scheme operator \mathcal{R} projects the integral to a fixed scale $x = 1$. The scale $x = 1$ or $p^2 = \mu^2$, fulfilling eq. (2.7), is called kinematic renormalization point. The MS-scheme also involves a scale μ in the definition of $x = p^2/\mu^2$, but the renormalized Green function $\hat{G}_{\mathcal{R}}(\alpha, x)$ will be unity at some other scale $p^2 = \hat{\mu}^2 = \delta(\alpha) \cdot \mu^2$, where the factor $\delta(\alpha)$ is itself a function of α .

All quantities computed in minimal subtraction are denoted with hat like $\hat{G}_{\mathcal{R}}$. We denote MS-bar quantities with a bar like $\bar{G}_{\mathcal{R}}$. The undecorated quantities like $G_{\mathcal{R}}$ are in the MOM-scheme.

For a primitively divergent 1-scale Feynman graph in dimensional regularization, the UV-pole essentially equals the coefficient of the logarithmic term in the external momentum. Consequently, the derivative with respect to momentum and the pole-part of the counter term are not independent. For the all-order Green function, this relation translates to a relation between the anomalous dimension and the Z -factor. Such relations have long been known in the traditional formulation ("Gross-'t Hooft relations") [1, 15, 23] as well as in the Hopf-algebraic formulation ("scattering

type formula”) of quantum field theory [17],[18, Sec. 7]. In the case of a linear Dyson-Schwinger-Equation, the coupling is not renormalized and the anomalous dimension is given by the MS counter term

$$(2.8) \quad \gamma_1(\alpha) = \alpha \frac{d}{d\alpha} \left(\text{Res}_{\frac{1}{\epsilon}} \hat{Z}(\alpha, \epsilon) \right) \quad \text{or equivalently} \quad \gamma_1(\alpha) = \lim_{\epsilon \rightarrow 0} \frac{d}{d \ln \mu} \ln \hat{Z}(\alpha \mu^\epsilon, \epsilon).$$

2.3. Expansion in logarithms. The renormalized solution of a 1-scale DSE in MOM-renormalization with renormalization point $x = 1$ can be expanded in logarithms according to

$$(2.9) \quad G_{\mathcal{R}}(x) = 1 + \sum_{k=1}^{\infty} \gamma_k(\alpha) \ln(x)^k.$$

In a physical model, $x = p^2/\mu^2$ is the squared momentum, measured relative to some reference μ^2 . The derivative of the connected (not 1PI) 2-point-function $G_{\mathcal{R}}^{-1}$ with respect to the logarithmic momentum $\ln(\sqrt{x})$ at the renormalization point is called the anomalous dimension. In our convention this is $\gamma(\alpha) = -2\gamma_1(\alpha)$, but in what follows, we will simply call $\gamma_1(\alpha)$ the anomalous dimension. The functions $\gamma_{k>1}(\alpha)$ can be computed from the renormalization group equation [27], which implies for the expansion eq. (2.9), with invariant charge eq. (2.2),

$$(2.10) \quad k\gamma_k(\alpha) = \gamma_1(\alpha) (s\alpha\partial_\alpha + 1) \gamma_{k-1}(\alpha).$$

For a linear DSE, the exponent in the invariant charge eq. (2.2) is $s = 0$, and consequently one obtains $\gamma_k(\alpha) = \frac{1}{k!} \gamma_1^k$. This corresponds to a scaling solution $G_{\mathcal{R}}(x) = x^{\gamma_1(\alpha)}$. The anomalous dimension $\gamma_1(\alpha)$ itself fulfils a non-linear ODE given by inserting the RGE-operator eq. (2.10) into the Mellin transform of the primitive kernel[27, 34]:

$$(2.11) \quad \frac{1}{-u \cdot M(u)} \Big|_{u \rightarrow -\gamma_1(s\alpha\partial_\alpha + 1)} \gamma_1(\alpha) = \alpha.$$

This can be an ODE of infinite order, see appendix A for the Mellin transforms of our kernels. For a linear DSE with $s = 0$, it reduces to the algebraic equation $M(-\gamma_1(\alpha)) = \alpha^{-1}$ [26].

There is a second expansion of the renormalized Green function $G_{\mathcal{R}}(x)$ in terms of logarithms, the leading-log expansion. It is a reordering of eq. (2.9) in powers of $(\alpha \ln(x))$,

$$(2.12) \quad G_{\mathcal{R}}(\alpha, x) = 1 + \sum_{k=1}^{\infty} H_k(\alpha \ln(x)) \alpha^k.$$

The function $H_1(z)$ is the leading-log contribution to the Green function, and $H_k(z)$ represents the next-to^k leading log part. These expansions have been studied recently [29, 19, 28], one of the results being that for a DSE eq. (2.5) with invariant charge eq. (2.2) where $s \neq 0$ one has [28]

$$(2.13) \quad H_1(z) = (1 + sg_1z)^{-\frac{1}{s}}, \quad H_2(z) = \frac{(1 + sg_1z)^{-\frac{1}{s}-1}}{-sg_1} g_2 \ln(1 + sg_1z)$$

$$H_3(z) = \frac{(1 + sg_1z)^{-\frac{1}{s}-2}}{s^2 g_1^2} \left(s^2 g_1 z (g_2^2 - g_1 g_3) - sg_2^2 \ln(1 + sg_1z) + \frac{g_2^2}{2} (1 + s) \ln^2(1 + sg_1z) \right).$$

Here, $g_j = -[\alpha^j] \gamma_1$ is the j^{th} coefficient of $\gamma_1(\alpha)$. The limit $s \rightarrow 0$ exists, for the linear DSEs

$$(2.14) \quad H_1(z) = e^{-g_1 z}, \quad H_2(z) = -g_2 z e^{-g_1 z}, \quad H_3(z) = \frac{1}{2} (g_2^2 z - 2g_3) z e^{-g_1 z}.$$

2.4. Shifted renormalization point. The formulas of section 2.3 are valid for MOM renormalization at $x = 1$. Now choose a kinematic renormalization point $x = \delta^{-1} \neq 1$. This is equivalent to choosing a reference momentum $\mu' = \sqrt{\delta} \cdot \mu$ instead of μ and using a new variable $x' := p^2/\mu'^2$ such that $x = 1$ equals $x' = \delta^{-1}$. The equation $G_{\mathcal{R}}(x) = G_{\mathcal{R}}(\delta x') = G'_{\mathcal{R}}(x')$ implies for eq. (2.9)

$$(2.15) \quad G'_{\mathcal{R}}(x') = \gamma'_0(\alpha) + \sum_{k=1}^{\infty} \gamma'_k(\alpha) \ln(x')^k, \quad \gamma'_k = \sum_{j=k}^{\infty} \binom{j}{k} \gamma_j \ln(\delta)^{j-k}.$$

These new coefficients $\gamma'_k(\alpha)$ do not fulfill the renormalization group equation eq. (2.10), but instead

$$(2.16) \quad \gamma_1(\alpha) (1 + s\alpha\partial_\alpha) \gamma'_j(\alpha) = (j+1)\gamma'_{j+1}(\alpha) + (j+1)s\alpha\gamma_1(\alpha)\gamma'_{j+1}(\alpha)\partial_\alpha \ln(\delta(\alpha)).$$

If the shift δ of the renormalization point is independent of the coupling constant α , then the second summand vanishes and one almost retains eq. (2.10) with the only difference that again $\gamma_1(\alpha)$, not $\gamma'_1(\alpha)$, governs the recursion. This is because even for the transformed Green function, still $\gamma_1(\alpha)$ and not $\gamma'_1(\alpha)$ is the derivative at the (kinematic) renormalization point, $\partial_{\ln(x)} G'_{\mathcal{R}}(x)|_{x=\delta^{-1}} = \gamma_1(\alpha)$.

In the minimal subtraction (MS) scheme, the shift $\delta(\alpha)$ does depend on the renormalized coupling α . In that case eq. (2.16) can be used to find this dependence, for example, setting $j = 1$,

$$(2.17) \quad \frac{\partial}{\partial \alpha} \ln(\delta(\alpha)) = \frac{\gamma_1 \gamma'_1 - 2\gamma'_2}{2\gamma'_2 s \alpha} + \frac{1}{2\gamma'_2} \frac{\partial}{\partial \alpha} \gamma'_1 \quad (\text{for } s \neq 0).$$

This allows to compute $\delta(\alpha)$ up to the constant term.

For the shift from MOM- to MS-renormalization, the constant term is fixed by the first order solution. Let the primitive kernel Feynman integral of the DSE be $\Gamma = (f^{-1}\frac{1}{\epsilon} + f_0 + f_1\epsilon + \dots)x^\epsilon$. Then $\alpha\Gamma$ is the first-order solution of the DSE and the anomalous dimension in MOM is $\gamma_1 = -\alpha f_{-1} + \mathcal{O}(\alpha^2)$. On the other hand, in MS renormalization the value of $G_{\mathcal{R}}$ at $x = 1$ is $\hat{\gamma}_0 = 1 + \alpha f_0 + \mathcal{O}(\alpha^2)$. Using eq. (2.15), this fixes the constant term of $\ln(\delta(\alpha))$:

$$(2.18) \quad \ln(\delta(\alpha)) = -f_0(f_{-1})^{-1} + \mathcal{O}(\alpha).$$

Remarkably, $\delta(0) = e^{-f_0/f_{-1}} \neq 1$ unless $f_0 = 0$, so the shift does not necessarily vanish for vanishing coupling. This result does not depend on the invariant charge in the DSE, just on the kernel.

In the linear case, $s = 0$, the scaling solution x^{γ_1} is rescaled by a factor $\gamma'_0 \neq 1$, this means $x^{\gamma_1} = \gamma'_0 \cdot (x')^{\gamma_1}$. Therefore, $\delta(\alpha)$ can be computed directly. The order-zero-term matches eq. (2.18):

$$(2.19) \quad \delta(\alpha) = (\gamma'_0(\alpha))^{\frac{1}{\gamma_1(\alpha)}} = e^{-\frac{f_0}{f_{-1}}} + \mathcal{O}(\alpha) \quad (\text{for } s = 0).$$

3. LINEAR DSE IN $D = 4 - 2\epsilon$ DIMENSIONS

We first consider a linear Dyson-Schwinger-equation of iterated one-loop Feynman graphs, namely

$$(3.1) \quad \hat{G}_{\mathcal{R}}(q^2) = 1 + \lambda \int \frac{d^D k}{(2\pi)^D} \frac{\hat{G}_{\mathcal{R}}(k^2)}{(k+q)^2 k^2} - \hat{\mathcal{R}} \left[\lambda \int \frac{d^D k}{(2\pi)^D} \frac{\hat{G}_{\mathcal{R}}(k^2)}{(k+q)^2 k^2} \right].$$

Here, λ is a coupling constant and $D = 4 - 2\epsilon$ is the spacetime dimension. Equation (3.1) is the linear DSE (rainbow approximation) for the fermion propagator in Yukawa theory, but scaled and projected onto suitable tensors such that the order zero (tree level) solution is

$$(3.2) \quad \hat{G}_{\mathcal{R}}^{(0)}(q^2) := 1.$$

3.1. Computation of the coefficients. One can solve the DSE eq. (3.1) to first order by inserting eq. (3.2) into it and computing the integrals according to appendix B:

$$(3.3) \quad \hat{G}_{\mathcal{R}}^{(1)}(q^2) = 1 + \frac{\lambda}{(4\pi)^2} (1 - \hat{\mathcal{R}}) \left[(4\pi)^\epsilon e^{-\gamma_E \epsilon} \left(\frac{q^2}{m^2} \right)^{-\epsilon} \sum_{w=-1}^{\infty} f_w^{(0)} \epsilon^w \right].$$

Here, m^2 is an arbitrary mass scale introduced for dimensional reasons and the coefficients $f_w^{(k)}$ are given in eq. (B.2). The operator $\hat{\mathcal{R}}$ projects the pole part of this equation, which is $f_{-1}^{(0)} \epsilon^{-1}$. This pole part is independent of momenta as expected in a locally renormalizable theory.

For a systematic treatment of higher orders, it will be advantageous to include the counter term as a summand $\propto 1 = (q^2)^0$ into the solution. Define

$$\bar{g}_{1,w}^{(1)} := f_w^{(0)} \quad \bar{g}_{0,w}^{(1)} := \begin{cases} -f_{-1}^{(0)} & w = -1 \\ 0 & \text{else} \end{cases}$$

then the renormalized solution to order one, eq. (3.3), is

$$(3.4) \quad \hat{G}_{\mathcal{R}}^{(1)}(q^2) = 1 + \frac{\lambda}{(4\pi)^2} \sum_{t=0}^1 (4\pi)^{t\epsilon} e^{-\gamma_E t\epsilon} \left(\frac{q^2}{m^2} \right)^{-t\epsilon} \sum_{w=-1}^{\infty} \bar{g}_{t,w}^{(1)} \epsilon^w.$$

The factor $(4\pi)^{t\epsilon} e^{-\gamma_E t\epsilon}$ eventually produces finite contributions $\propto \gamma_E$ and $\propto \ln(4\pi)$. In MS renormalization, these terms are present in the finite part of $\hat{G}_{\mathcal{R}}$ while in MS-bar renormalization they are assigned to the counter term \bar{Z} and thus absent from $\bar{G}_{\mathcal{R}}$. To facilitate computations, we will absorb them into the momentum variable. This way, we effectively obtain the MS-bar Green function of the new momentum variable. On the other hand, our counter term will be \hat{Z} in MS as it does not contain the $\ln(4\pi), \gamma_E$ contributions either. At first, this might seem confusing, but it dramatically facilitates the computation as we can skip in every intermediate step two additional series expansions, the ones of $e^{-\gamma_E t\epsilon}$ and $e^{\ln(4\pi)t\epsilon}$. Let therefore

$$(3.5) \quad \hat{x} := \frac{q^2}{m^2}, \quad \bar{x} := \frac{e^{\gamma_E} q^2}{4\pi m^2} \equiv \frac{q^2}{\bar{m}^2}, \quad \hat{G}_{\mathcal{R}}(\hat{x}) \equiv \bar{G}_{\mathcal{R}}(\bar{x}).$$

The transition $\hat{x} \leftrightarrow \bar{x}$ is a rescaling of the momentum which can also be understood as choosing a suitable value of the reference momentum m , as evidenced by the second equal sign where $\bar{m}^2 = 4\pi e^{-\gamma_E} m^2$. This is not kinematic renormalization: m merely tells how we measure momenta, the MS-renormalized Green function $\hat{G}_{\mathcal{R}}(q^2)$ does not fulfil any particular condition at the point $q^2 = m^2$. Also, m^2 is not the mass of a particle, the field is still massless. Finally, let $\alpha := \lambda(4\pi)^{-2}$.

Higher orders of the renormalized Green function are computed iteratively. Assume that we know the solution to order $(m-1)$,

$$\bar{G}_{\mathcal{R}}^{(m-1)}(\bar{x}) = \bar{G}_{\mathcal{R}}^{(m-2)}(\bar{x}) + \alpha^{m-1} \sum_{t=0}^{m-1} (\bar{x})^{-t\epsilon} \sum_{w=-(m-1)}^{\infty} \bar{g}_{t,w}^{(m-1)} \epsilon^w.$$

Inserting this into eq. (3.1), the order m solution is

$$(3.6) \quad \bar{G}_{\mathcal{R}}^{(m)}(\bar{x}) = \bar{G}_{\mathcal{R}}^{(m-1)}(\bar{x}) + \alpha^m \sum_{t=0}^m (\bar{x})^{-t\epsilon} \sum_{w=-m}^{\infty} \bar{g}_{t,w}^{(m)} \epsilon^w,$$

where the new coefficients are determined by

$$(3.7) \quad \bar{g}_{u,w}^{(m)} := \sum_{n=-m+1}^{w+1} \bar{g}_{u-1,n}^{(m-1)} f_{w-n}^{(u-1)} \quad \forall u > 0.$$

The counter term is included in this sum as the $t = 0$ summand. The coefficient of order ϵ^w in the MS-counter term at m loops is

$$(3.8) \quad \bar{g}_{0,w}^{(m)} = - \sum_{u=1}^m \bar{g}_{u,w}^{(m)} \quad \text{if } w \in \{-m, \dots, -1\}, \text{ and } \bar{g}_{0,w}^{(m)} = 0 \text{ for all other } w.$$

The all-order perturbative solution $\bar{G}_{\mathcal{R}}(\bar{x})$ of eq. (3.1) is defined as the limit $m \rightarrow \infty$ in eq. (3.6), effectively it is an infinite sum over the orders α^m in the coupling. We exchange the sums to expose the expansion eq. (2.9) and the counter term \hat{Z} :

$$(3.9) \quad \bar{G}_{\mathcal{R}}(\bar{x}) = \hat{Z}(\alpha, \epsilon) + \sum_{k=0}^{\infty} \ln(\bar{x})^k \sum_{t=1}^{\infty} \frac{(-t)^k}{k!} \sum_{m=t}^{\infty} \alpha^m \sum_{w=-m}^{\infty} \bar{g}_{t,w}^{(m)} \epsilon^{k+w}.$$

As explained above eq. (3.5), we have introduced the MS (not MS-bar) counter term,

$$(3.10) \quad \hat{Z}(\alpha, \epsilon) := 1 + \sum_{m=1}^{\infty} \alpha^m \sum_{w=-m}^{-1} \bar{g}_{0,w}^{(m)} \epsilon^w = 1 - \sum_{m=1}^{\infty} \alpha^m \sum_{w=-m}^{-1} \sum_{t=1}^m \bar{g}_{t,w}^{(m)} \epsilon^w.$$

The eqs. (3.9) and (3.10) together with the recursion relations eqs. (3.7) and (3.8) allow us to compute the solution of the DSE 3.1 to arbitrary order.

A similar procedure can be used to obtain the MOM-renormalized finite Green function $G_{\mathcal{R}}(\bar{x})$. One merely has to extend eq. (3.7) to include all orders w of ϵ . If we are only interested in the finite (as $\epsilon \rightarrow 0$) part, then, in a linear DSE, it is sufficient to include the $w = 0$ term into the counter term. To this end, instead of eqs. (3.7) and (3.8) one uses

$$(3.11) \quad g_{u,w}^{(m)} := \begin{cases} \sum_{n=-m+1}^{w+1} g_{u-1,n}^{(m-1)} f_{w-n}^{(u-1)} & \forall u > 0 \\ - \sum_{u=1}^m g_{u,w}^{(m)} & \text{if } u = 0 \text{ and } w \in \{-m, \dots, 0\}, \text{ and } 0 \text{ else.} \end{cases}$$

The counter term computed by eq. (3.11) is not the “true” counter term of kinematic renormalization. But this prescription produces a MOM-renormalized finite Green function

$$(3.12) \quad G_{\mathcal{R}}(\bar{x}) = Z(\alpha, \epsilon) + \sum_{k=0}^{\infty} \ln(\bar{x})^k \frac{1}{k!} \sum_{m=t}^{\infty} \alpha^m \sum_{t=1}^{\infty} (-t)^k \sum_{w=-m}^{\infty} g_{t,w}^{(m)} \epsilon^{k+w}$$

which by construction takes the value unity at the renormalization point $\bar{x} = 1$, i.e. at the momentum $q^2 = \mu^2$. Now the interpretation of μ^2 has changed: In the MS- or MS-bar-solutions, it was an arbitrary momentum scale without any particular meaning for the Green function while in MOM it is the momentum where $G_{\mathcal{R}}(q^2) = 1$.

3.2. Renormalized correlation function. In MOM renormalization, the analytic solution of the linear DSE has long been known [21]. As always for a linear DSE, it is a pure scaling solution where the anomalous dimension $\gamma_1(\alpha)$ is determined from the Mellin transform of the primitive, see eq. (2.11) and appendix A. With the notation of eq. (2.9), the MOM-solution at $\epsilon = 0$ reads

$$(3.13) \quad G_{\mathcal{R}}(\bar{x}) = (\bar{x})^{\gamma_1(\alpha)}$$

where $\gamma_0(\alpha) = 1$, $\gamma_1(\alpha) = \frac{\sqrt{1-4\alpha}-1}{2} = - \sum_{n=1}^{\infty} C_{n-1} \alpha^n$, $\gamma_k(\alpha) = \frac{1}{k!} (\gamma_1(\alpha))^k$.

Here, C_n are the Catalan numbers. It has been verified symbolically up to order α^{25} that the series eq. (3.12) indeed coincides with eq. (3.13) in the limit $\epsilon \rightarrow 0$.

In MS-bar-renormalization, there is a finite remainder term in the ϵ^0 -coefficient of each order in α , which would have been subtracted in kinematic renormalization. Therefore, the MS-bar-coefficients $\bar{\gamma}_k(\alpha)$ in eq. (2.9) are generally different from the MOM-coefficients $\gamma_k(\alpha)$, see section 2.4. In order

to compute $\delta(\alpha)$, the shift of the renormalization point, according to eq. (2.19), we need to know $\bar{\gamma}_0(\alpha)$, the value of $\bar{G}_{\mathcal{R}}(\bar{x} = 1)$. From eq. (3.9) one reads off

$$(3.14) \quad \bar{\gamma}_0(\alpha) = 1 + \sum_{m=1}^{\infty} \alpha^m \sum_{t=1}^m \bar{g}_{t,0}^{(m)} = 1 + 2\alpha + \frac{11}{2}\alpha^2 + \frac{51 - 2\zeta(3)}{3}\alpha^3 + \frac{1341 - 80\zeta(3)}{24}\alpha^4 + \mathcal{O}(\alpha^5).$$

We have used that the \hat{Z} -factor in MS has, at finite order, only terms singular in ϵ and therefore does not contribute to $\bar{\gamma}_k$ and the summand $t = 0$ can be left out. For the interpretation as a change of renormalization point, the remaining functions $\bar{\gamma}_k(\alpha)$ have to be consistent with eqs. (2.15) and (3.13). It has been verified to order α^{25} and for $k \leq 15$ that indeed $\bar{\gamma}_k(\alpha) = \bar{\gamma}_0(\alpha) \cdot \gamma_k(\alpha)$.

Remarkably, for the linear DSEs considered here, it is possible to find a closed formula for $\bar{\gamma}_0(\alpha)$. To do this, one computes the logarithm of the series eq. (3.14) and repeatedly uses the OEIS [33]. One can first identify the rational coefficients and their generating function. Subtracting that part one is left with

$$\begin{aligned} \ln(\bar{\gamma}_0) - \ln\left(\frac{1 - \sqrt{1 - 4\alpha}}{2\alpha(1 - 4\alpha)^{\frac{1}{4}}}\right) &= -\zeta(3) \left(2\frac{\alpha^3}{3} + 8\frac{\alpha^4}{4} + 30\frac{\alpha^5}{5} + 112\frac{\alpha^6}{6} + 420\frac{\alpha^7}{7} + 1584\frac{\alpha^8}{8} + \dots\right) \\ &\quad - \zeta(5) \left(2\frac{\alpha^5}{5} + 12\frac{\alpha^6}{6} + 56\frac{\alpha^7}{7} + 240\frac{\alpha^8}{8} + 990\frac{\alpha^9}{9} + \dots\right) - \zeta(7) \dots \end{aligned}$$

At least up to $\zeta(11)$ and α^{25} , the coefficients of $\frac{\alpha^{j+m-1}}{j+m-1}$ in the term proportional to $\zeta(m)$ are given by the binomial coefficient $2^{\binom{2j+m-3}{j-1}}$. Assuming again that this holds universally, all series over α and then the remaining series in $\zeta(m)$ can be summed and yield known functions. The result is

$$(3.15) \quad \bar{\gamma}_0(\alpha) = e^{\gamma_E(1 - \sqrt{1 - 4\alpha})} \frac{1 - \sqrt{1 - 4\alpha}}{2\alpha(1 - 4\alpha)^{\frac{1}{4}}} \frac{\Gamma\left(\frac{3}{2} - \frac{1}{2}\sqrt{1 - 4\alpha}\right)}{\Gamma\left(\frac{1}{2} + \frac{1}{2}\sqrt{1 - 4\alpha}\right)} = \frac{-\gamma_1}{\alpha} \sqrt{\frac{d(-\gamma_1)}{d\alpha}} e^{-2\gamma_1\gamma_E} \frac{\Gamma(1 - \gamma_1)}{\Gamma(1 + \gamma_1)}.$$

In the latter form, $\gamma_1 \equiv \gamma_1(\alpha)$ is the anomalous dimension from eq. (3.13).

With this function $\bar{\gamma}_0(\alpha)$ and eq. (3.13), the MS-bar-renormalized solution $\bar{G}_{\mathcal{R}}(\bar{x})$ in the limit $\epsilon \rightarrow 0$ reads explicitly

$$(3.16) \quad \bar{G}_{\mathcal{R}}(\bar{x}) = \bar{\gamma}_0(\alpha) \cdot G_{\mathcal{R}}(\bar{x}) = \bar{\gamma}_0(\alpha) \cdot \bar{x}^{\gamma_1(\alpha)}.$$

From eq. (3.5) one can reconstruct the MS-renormalized function $\hat{G}_{\mathcal{R}}(\hat{p}^2)$:

$$(3.17) \quad \hat{G}_{\mathcal{R}}(\hat{x}) = \bar{G}_{\mathcal{R}}\left(\frac{\hat{x}}{4\pi e^{-\gamma_E}}\right) = \hat{\gamma}_0(\alpha) \cdot \hat{x}^{\gamma_1(\alpha)} \quad \text{where} \quad \hat{\gamma}_0(\alpha) := (4\pi e^{-\gamma_E})^{-\gamma_1(\alpha)} \cdot \bar{\gamma}_0(\alpha)$$

Following section 2.4, the correspondence between MS-, MS-bar- and MOM-renormalized Green functions can equivalently be expressed by their respective renormalization points. Let μ be the mass scale in MS- and MS-bar-renormalization. Then the Green function is unity at $x = \hat{\delta}^{-1}$ and $x = \bar{\delta}^{-1}$, respectively. Equivalently, $\hat{\mu}^2 = \hat{\delta} \cdot \mu^2$ and $\bar{\mu}^2 = \bar{\delta} \cdot \mu^2$ are the mass scales one needs to choose for MS and MS-bar, in order to reproduce kinematic renormalization at the scale μ^2 :

$$G_{\mathcal{R}}\left(\frac{q^2}{\mu^2}\right) \equiv \bar{G}_{\mathcal{R}}\left(\frac{q^2}{\bar{\mu}^2}\right) \equiv \hat{G}_{\mathcal{R}}\left(\frac{q^2}{\hat{\mu}^2}\right).$$

By eqs. (2.19), (3.13) and (3.15), these scales are related via

$$(3.18) \quad \bar{\delta}(\alpha) = \bar{\gamma}_0^{\frac{1}{\gamma_1}} = e^{-2} \left(1 - \frac{3}{2}\alpha - \left(\frac{49}{24} - \frac{2}{3}\zeta(3)\right)\alpha^2 + \mathcal{O}(\alpha^3)\right), \quad \hat{\delta}(\alpha) = \hat{\gamma}_0^{\frac{1}{\gamma_1}} = \frac{\bar{\delta}(\alpha)}{\sqrt{4\pi e^{-\gamma_E}}}.$$

The latter of course reproduces the transformation $m \leftrightarrow \bar{m}$ in eq. (3.5). The zeroth order coefficient is e^{-2} as expected from eq. (2.19) where $f_{-1} = f_{-1}^{(0)} = 1$, $f_0 = f_0^{(0)} = 2$. In any case, the shift between renormalization schemes is a finite function as long as $\alpha < \frac{1}{4}$, shown in fig. 1.

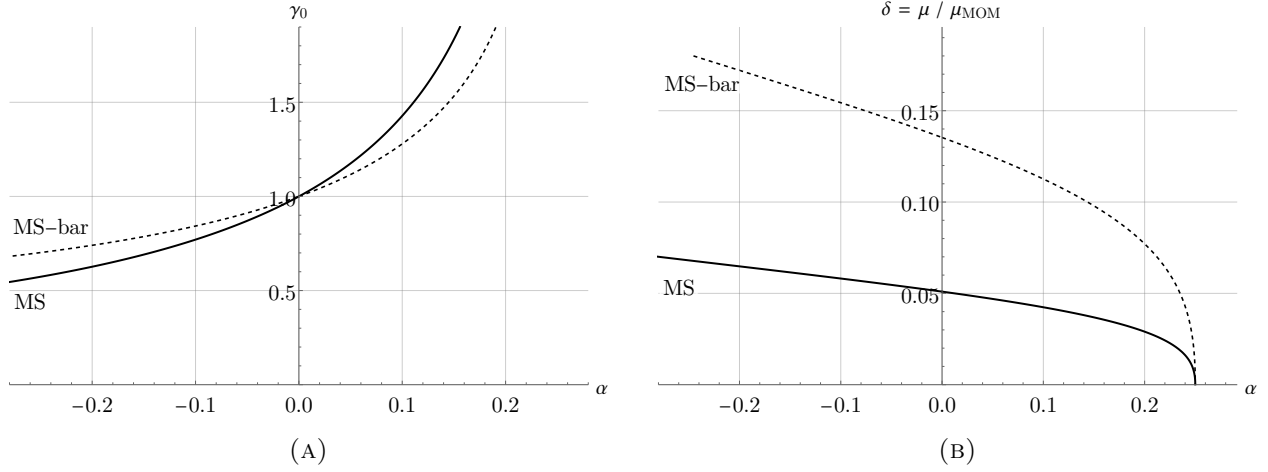


FIGURE 1. (A) Behaviour of the MS scaling-function $\hat{\gamma}_0(\alpha)$ (thick) and the MS-bar scaling function $\bar{\gamma}_0(\alpha)$ (dashed) as functions of the renormalized coupling α . Both are unity at $\alpha = 0$ and diverge at $\alpha = \frac{1}{4}$. (B) Rescaling factor $\delta(\alpha)$ according to section 2.4 of the reference momentum in MS-renormalization $\hat{\mu}$ (thick) and MS-bar-renormalization $\bar{\mu}$ (dashed) relative to the MOM-renormalization-point μ . The functions are equal up to the factor $\sqrt{4\pi e^{-\gamma_E}}$. They are not unity for $\alpha = 0$.

3.3. Counter term. It turns out that not only the finite parts, but also the counter term can be summed explicitly in the linear DSE 3.1 in MS. Its coefficients are defined by eq. (3.10). $\hat{Z}(\alpha, \epsilon)$ is a power series in α and $\frac{1}{\epsilon}$, but the logarithm is just proportional to $\frac{1}{\epsilon}$:

$$\ln \left(\hat{Z}(\alpha, \epsilon) \right) = -\frac{1}{\epsilon} \left(\alpha + \frac{\alpha^2}{2} + 2\frac{\alpha^3}{3} + 5\frac{\alpha^4}{4} + 14\frac{\alpha^5}{5} + 42\frac{\alpha^6}{6} + \dots \right).$$

Once more we recognize the Catalan numbers and introduce $\gamma_1 = \gamma_1(\alpha)$ from eq. (3.13),

$$(3.19) \quad \hat{Z}(\alpha, \epsilon) = \exp \left(-\frac{1}{\epsilon} \sum_{m=1}^{\infty} C_{n-1} \frac{\alpha^n}{n} \right) = e^{-\frac{1}{\epsilon} \left(1 - \sqrt{1-4\alpha} + \ln \left(1 - \frac{1-\sqrt{1-4\alpha}}{2} \right) \right)} = e^{\frac{1}{\epsilon} (2\gamma_1 - \ln(1+\gamma_1))}.$$

As long as α and ϵ have the same sign, this function has the limit $\hat{Z}(\alpha, 0^+) = 0$ when $\epsilon \rightarrow 0$, see fig. 2. With eq. (3.19), the counter term turns out to be a remarkably well-behaved function of ϵ , compared to its perturbative expansion, where every single term diverges as $\epsilon \rightarrow 0$.

We write for the counter term of a linear DSE in any renormalization scheme the expansion

$$(3.20) \quad Z(\alpha, \epsilon) \equiv \exp \left(- \sum_{n=-1}^{\infty} z_n(\alpha) \cdot \epsilon^n \right).$$

In the MS scheme, all $z_{n \geq 0}(\alpha)$ vanish identically and the only remaining function is

$$(3.21) \quad z_{-1}(\alpha) = -[\epsilon^{-1}] \ln Z = - \int_0^\alpha \frac{du}{u} \gamma_1(u) \quad \Rightarrow \quad \hat{Z}(\alpha, \epsilon) = \exp \left(\frac{1}{\epsilon} \int_0^\alpha \frac{\gamma_1(u)}{u} du \right).$$

It has been confirmed explicitly to order α^{20} that $z_{-1}(\alpha)$ takes this form in all considered renormalization schemes, as suggested by eq. (2.8).

It is clear from the construction eq. (3.11) that different renormalization schemes amount to different ways to assign the non-singular parts of the amplitude to $G_{\mathcal{R}}$ or to Z , respectively. Specifically, in MOM-renormalization the quantity γ_0 is unity. It is computed via eq. (3.14), but this time the summand $t = 0$ is not zero and needs to be included into the sum. Consequently, the scaling factor $\bar{\gamma}_0(\alpha)$, which in MS is present in $G_{\mathcal{R}}$, appears in MOM in the Z -factor eq. (3.20),

$$(3.22) \quad z_0 = -[\epsilon^0] \ln Z = \ln \bar{\gamma}_0(\alpha).$$

In our pseudo-MOM-scheme eq. (3.11), all other $z_{n>0}$ vanish. In true kinematic renormalization, they are present. The author computed the coefficients $z_{n\leq 9}$ up to order α^{10} but did not succeed in finding generating functions. However it turned out that all $z_{n\leq 9}(\alpha)$ for $0 < \alpha < \frac{1}{4}$ are, within the computed order, strictly positive. This implies that the exponent is strictly negative for all $\epsilon > 0$ and hence $Z(\alpha, \epsilon) \in [0, 1]$. The classical interpretation of the Z -factor as a probability requires these bounds. Compare [25, Sec 8] for the various interpretations of Z and their relations.

This discussion of the counter term is not only entertaining, but in a linear DSE the formula eq. (3.22) in principle allows for an ab-initio computation of $\bar{\gamma}_0(\alpha)$ and hence $\delta(\alpha)$. Namely, if one were to know the solution $G_{\mathcal{R}}(p^2, \epsilon)$ of the Dyson-Schwinger-equation exactly for finite $\epsilon \neq 0$ then

$$(3.23) \quad Z(\alpha, \epsilon) = 1 - (4\pi)^2 \alpha \int \frac{d^D k}{(2\pi)^D} \frac{G_{\mathcal{R}}(k^2)}{(k + \mu)^2 k^2} \Big|_{\mu^2=1}.$$

Unfortunately it is not sufficient to just insert the $D = 4$ solution eq. (3.13) into the D -dimensional integral. At least, eq. (3.23) guarantees, using eqs. (2.11) and (3.13), that $Z(\alpha, \epsilon) = 0 + \mathcal{O}(\epsilon)$ in kinematic renormalization. This is in line with [30] and a comment made in [26]: The all-order-solution eq. (3.13) “regulates itself” by its anomalous dimension. The integral in the DSE eq. (3.1) is not divergent and the remaining finite counter term is set to zero by choice of the renormalization point. Figure 2 shows how \hat{Z} approaches zero as the scaling solution $\epsilon = 0$ is reached.

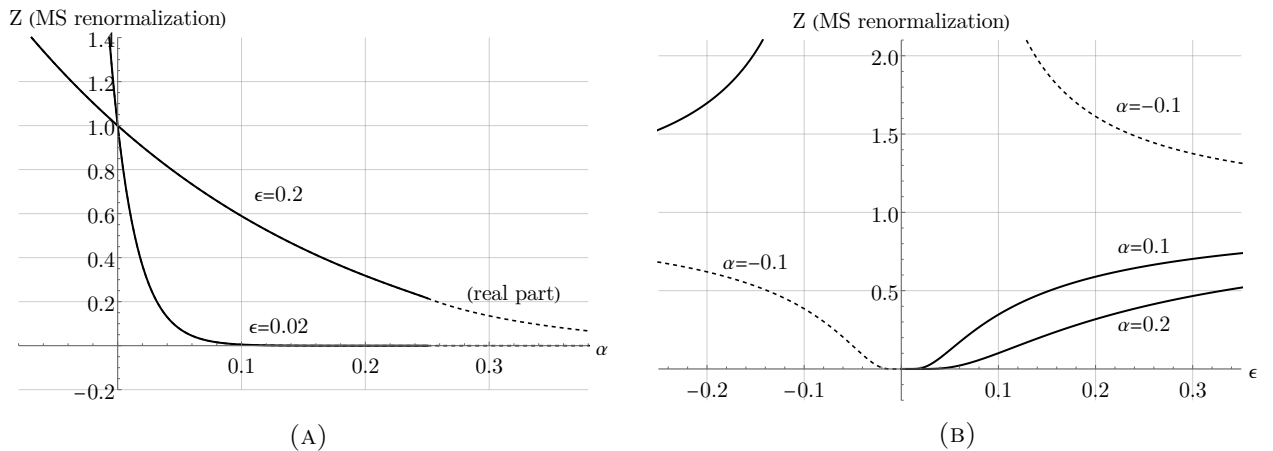


FIGURE 2. (A) Counter term $\hat{Z}(\alpha, \epsilon)$ in MS as a function of the renormalized coupling α for different values of ϵ . As $\epsilon \rightarrow 0^+$, the function approaches zero for $\alpha > 0$ and diverges for $\alpha < 0$. For $\alpha > \frac{1}{4}$, the counter term acquires an imaginary part which is not shown. (B) The same counter term as a function of ϵ for fixed values of α . For positive α , the counter term smoothly approaches the value zero as $\epsilon \rightarrow 0^+$.

4. LINEAR DSE IN $D = 6 - 2\epsilon$ DIMENSIONS

For the 6-dimensional case, the procedure is completely analogous to the one described in the previous section. We will use the same symbols as in the $D = 4$ case in order to not clutter notation.

The Dyson-Schwinger-equation is once more eq. (3.1), only now with $D = 6 - 2\epsilon$. This time, we define $\alpha := \lambda(4\pi)^{-3}$ to account for the additional factor 4π produced by the integration. Moreover, the 1-loop-integral is now proportional to q^2 but this factor is absorbed by projection onto the basis tensor such that again the tree level solution is $G_{\mathcal{R}}^{(0)}(q^2) = 1$. Then, the coefficients of the renormalized Green function and the counter term are given by the same recursion relations as above, namely eqs. (3.7), (3.8) and (3.11). The crucial difference is that for $f_n^{(k)}$ one now takes the value of the 6-dimensional primitive integral, as given in eq. (B.3).

Once more, the anomalous dimension can be computed analytically from the Mellin transform of the 1-loop integral appendix A. The Green function in kinematic renormalization is [20]

$$G_{\mathcal{R}}(\bar{x}) = (\bar{x})^{\gamma_1(\alpha)}, \quad \gamma_1(\alpha) = \frac{\sqrt{5 + 4\sqrt{1 + \alpha}} - 3}{2}.$$

The functions $\bar{\gamma}_k(\alpha)$ are again computed from eq. (3.9) using the appropriate $\bar{g}_{t,s}^{(m)}$. Like above, all $\bar{\gamma}_k(\alpha)$ are proportional to the corresponding $\gamma_k(\alpha)$ at least up to α^{25} and $k = 20$.

The series coefficients of $\bar{\gamma}_0(\alpha)$ can no longer be identified from tables right away but the result eq. (3.15), expressed in terms of $\gamma_1(\alpha)$, is a helpful starting point. Eventually, one arrives at

$$(4.1) \quad \bar{\gamma}_0(\alpha) = 3\sqrt{3} \frac{e^{\frac{1}{2}(\sqrt{5+4\sqrt{1+\alpha}}-3)(1-2\gamma_E)} \left(\sqrt{5+4\sqrt{1+\alpha}}-3\right) \Gamma\left(\frac{5}{2}-\frac{1}{2}\sqrt{5+4\sqrt{1+\alpha}}\right)}{\alpha \left((1+\alpha)(5+4\sqrt{1+\alpha})\right)^{\frac{1}{4}} \Gamma\left(-\frac{1}{2}+\frac{1}{2}\sqrt{5+4\sqrt{1+\alpha}}\right)}$$

$$= \frac{6\gamma_1}{\alpha} \sqrt{\frac{d(6\gamma_1)}{d\alpha}} e^{\gamma_1(1-2\gamma_E)} \frac{\Gamma(1-\gamma_1)}{\Gamma(1+\gamma_1)}.$$

This has been verified symbolically to order α^{25} . Knowing $\bar{\gamma}_0(\alpha)$, the shifts between MS-bar- resp. MS- and MOM-renormalization are $\bar{\delta}(\alpha) = \bar{\gamma}_0^{\frac{1}{\alpha}}$ and $\hat{\delta}(\alpha) = (4\pi e^{-\gamma_1})^{-\frac{1}{2}} \bar{\delta}(\alpha)$.

The counter term in MS for the 6-dimensional theory is

$$\hat{Z}(\alpha, \epsilon) = e^{\frac{1}{\epsilon} \left(2\sqrt{5+4\sqrt{1+\alpha}} - 6 - \frac{3}{2} \ln(\alpha) + \ln(108) + \frac{1}{2} \ln \frac{\sqrt{5+4\sqrt{1+\alpha}}-1}{\sqrt{5+4\sqrt{1+\alpha}}+1} + \frac{3}{2} \ln \frac{\sqrt{5+4\sqrt{1+\alpha}}-3}{\sqrt{5+4\sqrt{1+\alpha}}+3} \right)}.$$

This function fulfills eq. (3.21). Furthermore, it has been checked to order α^{25} resp. α^{10} that $Z(\alpha, \epsilon)$ reproduces $\bar{\gamma}_0$ via eq. (3.22) for the pseudo-MOM and the true MOM scheme, respectively.

5. KREIMER'S LINEAR TOY MODEL

Both Dyson-Schwinger-Equations considered above were based on the same 1-loop primitive Feynman graph as an integral kernel. Our formalism is not restricted to that particular integral, for comparison we here examine the linear Dyson-Schwinger-equation in a toy model of renormalization proposed by Dirk Kreimer [31]. It reads

$$(5.1) \quad \hat{G}_{\mathcal{R}}(x) = 1 + \left(1 - \hat{\mathcal{R}}\right) \alpha \int_0^\infty \frac{dy (xy)^{-\epsilon}}{1+y} \hat{G}_{\mathcal{R}}(xy),$$

where again ϵ is a regularization parameter. There is no distinction between MS- and MS-bar schemes in the toy model. We retreat to a comparison between MS and pseudo-MOM, where the

the coefficients of the former are computed via

$$\hat{g}_{u,w}^{(m)} = \sum_{n=-m+1}^{w+1} \hat{g}_{u-1,n}^{(m-1)} f_{w-n}^{(u-1)}, \quad \hat{g}_{0,w}^{(m)} = - \sum_{u=1}^m \hat{g}_{u,w}^{(m)} \quad \text{for } w < 0.$$

For pseudo MOM-renormalization, we once more modify $g_{0,w}^{(m)}$ according to eq. (3.11).

The anomalous dimension, computed from the Mellin transform eq. (2.11) and appendix A, is

$$\gamma_1(\alpha) = -\frac{1}{\pi} \arcsin(\pi\alpha) = -\alpha - \frac{\pi^2}{6}\alpha^3 - \frac{3\pi^4}{40}\alpha^5 - \frac{5\pi^6}{112}\alpha^7 - \dots$$

It has been verified to order α^{30} that the symbolic calculation of $G_{\mathcal{R}}(x)$ in pseudo-MOM renormalization produces, in the limit $\epsilon \rightarrow 0$, the expansion coefficients of $x^{\gamma_1(\alpha)}$.

For MS, using [33, A034255], the scaling factor is

$$(5.2) \quad \hat{\gamma}_0(\alpha) = 1 + \sum_{m=1}^{\infty} \alpha^m \sum_{t=1}^m \hat{g}_{t,0}^{(m)} = 1 + \left(\frac{\pi^2\alpha^2}{4}\right) + \frac{5}{2} \left(\frac{\pi^2\alpha^2}{4}\right)^2 + \dots = (1 - \pi^2\alpha^2)^{-\frac{1}{4}} = \sqrt{\frac{d}{d\alpha} \gamma_1}.$$

From this, the change of the renormalization point can be computed using eq. (2.19). One finds

$$\ln(\hat{\delta}(\alpha)) = \frac{\pi \ln(1 - \alpha^2\pi^2)}{4 \arcsin(\alpha\pi)} = -\frac{\pi^2}{4}\alpha - \frac{\pi^4}{12}\alpha^3 - \frac{73\pi^6}{1440}\alpha^5 - \mathcal{O}(\alpha^7),$$

where the constant coefficient vanishes since for the toy model $f_0 = f_0^{(0)} = 0$.

The series coefficients of the toy model are somewhat easier than for the physical theory. This entails that in the expansion

$$(5.3) \quad Z(\alpha, \epsilon) \equiv \exp\left(-\sum_{n=-1}^{\infty} z_n(\alpha) \cdot \epsilon^n\right) \equiv \exp\left(\sum_{n=1}^{\infty} z'_n(\epsilon) \cdot \alpha^n\right).$$

the functions $z_n(\alpha)$ and $z'_n(\alpha)$ can be found symbolically. Some of them are quoted in appendix C for the interested reader. They suggest that $Z(\alpha, \epsilon) \in [0, 1]$. As expected in eq. (2.8), also the linear toy model fulfils

$$z_{-1} = -[\epsilon^{-1}] \ln Z = -\int_0^{\alpha} \frac{du}{u} \gamma_1(u), \quad z_0 = -[\epsilon^0] \ln Z = -\frac{1}{4} \ln(1 - \alpha^2\pi^2) = \ln \bar{\gamma}_0(\alpha).$$

6. NON-LINEAR DSE IN $D = 4$

In the remainder of this paper we repeat the above analysis of the two physical models and the toy model for the case that the Dyson-Schwinger-Equation is non-linear. Namely, instead of $Q \equiv 1$ we insert the invariant charge eq. (2.2),

$$(6.1) \quad Q(G(\alpha, x)) = (G(\alpha, x))^s,$$

where $s \in \{-5, \dots, +5\}$. It seems that the literature so far has mostly concentrated on the physically most relevant cases $s = 0$ (linear approximation, e.g. [21, 20, 26]) and $s = -2$ (one inverse Green function inserted into the kernel, e.g. [12, 13, 6, 5, 7, 11, 9]). In our case, the corresponding power of $G_{\mathcal{R}}$ is inserted into *only one* edge of the primitive. The setup discussed in [6, 5, 7] is conceptually different from our $s = -3$ since it amounts to inserting one $G_{\mathcal{R}}^{-2}$ into each of the two internal edges. Compare our result eq. (6.6) with [6, Table 1]. Also see [34, Sec. 5] for a discussion how insertion into only a subset of the available edges is equivalent to including additional primitive kernels.

6.1. Computation of the coefficients. The MS-renormalized Dyson-Schwinger-Equation for the $D = 4$ model reads

$$(6.2) \quad \hat{G}_{\mathcal{R}}(q^2) = 1 + \alpha(4\pi)^2 (1 - \hat{\mathcal{R}}) \int \frac{d^D k}{(2\pi)^D} \frac{(\hat{G}_{\mathcal{R}}(k^2))^{s+1}}{(k+q)^2 k^2}.$$

Note that as above we choose a sign $+\alpha$ in front of the integral.

For a recursive computation of the coefficients, we once more introduce \hat{x}, \bar{x} according to eq. (3.5) and thereby switch from MS- to MS-bar-renormalization. The first order solution coincides with the one of the linear DSE, eq. (3.4),

$$\bar{G}_{\mathcal{R}}^{(1)}(\bar{x}) = 1 + \alpha \sum_{t=0}^1 \bar{x}^{-t\epsilon} \sum_{w=-1}^{\infty} \bar{g}_{t,w}^{(1)} \epsilon^w.$$

The index (m) in the linear case counts both the coradical degree (= number of recursive iteration of the solution) and the order in α (= loop number of the involved graphs). In the non-linear DSE, we truncate the series expansion of $(\hat{G}_{\mathcal{R}}(k^2))^{s+1}$ at order α^{m-1} so that $\hat{G}_{\mathcal{R}}^{(m)}(q^2)$ again involves Graphs with at most m loops. This choice is arbitrary but convenient because it saves one index.

The recursion formula for the next order is more complicated than in the linear case section 3.1. This is because the non-linear DSE eq. (6.2) involves a non-trivial power of the Green function inside the integral which needs to be expanded both in α and in $\bar{x}^{-\epsilon}$. Assume we know the order- m -solution in the form

$$\bar{G}_{\mathcal{R}}^{(m)}(\bar{x}) = 1 + \sum_{n=1}^m \alpha^n \sum_{u=0}^n \bar{x}^{-u\epsilon} \sum_{s=-n}^{\infty} \bar{g}_{u,w}^{(n)} \epsilon^w =: 1 + \sum_{n=1}^m \alpha^n \bar{G}_n(\bar{x}, \epsilon),$$

where we defined functions $\bar{G}_n(\bar{x}, \epsilon)$. They are universal for all m . Next, we write a generic expansion of the invariant charge eq. (6.1) according to

$$(6.3) \quad \bar{G}^{(m)}(\alpha, \bar{x}) \cdot Q(\bar{G}^{(m)}(\bar{x})) \equiv \left(\bar{G}_{\mathcal{R}}^{(m)}(\bar{x}) \right)^{s+1} =: 1 + \sum_{n=1}^m \alpha^n \sum_{t=0}^n \bar{x}^{-t\epsilon} \bar{h}_t^{(n)}(\epsilon).$$

The helper functions $\bar{h}_t^{(n)}(\epsilon)$ are Laurent series in ϵ with the highest pole order ϵ^{-n} . They are given by Faa di Bruno's formula and the Binomial theorem, $B_{n,k}$ are Bell polynomials[4] [16, p 134]:

$$(6.4) \quad \frac{1}{\left(\bar{G}_{\mathcal{R}}^{(m)}(\bar{x}) \right)^{-s-1}} = \frac{1}{(-s-2)!} \sum_{n=0}^{\infty} \alpha^n \frac{1}{n!} \sum_{k=1}^n (-s-2+k)! B_{n,k} (1! \bar{G}_1, 2! \bar{G}_2, \dots), \quad s < -1$$

$$\left(\bar{G}_{\mathcal{R}}^{(m)}(\bar{x}) \right)^{s+1} = (s+1)! \sum_{n=0}^{\infty} \alpha^n \frac{1}{n!} \sum_{k=0}^{s+1} \frac{1}{(s+1-k)!} B_{n,k} (1! \bar{G}_1, 2! \bar{G}_2, \dots), \quad s > -1.$$

Knowing the functions $\bar{h}_t^{(n)}(\epsilon)$, one integrates the sum eq. (6.3) term-wise like in the linear case section 3.1 and obtains the next-order coefficients

$$\bar{g}_{1,w}^{(1)} = f_w^{(0)}, \quad \bar{g}_{u,w}^{(n)} = \sum_{r=-1}^{n+w-1} \left([\epsilon^{w-r}] \bar{h}_{u-1}^{(n-1)} \right) f_r^{(u-1)}.$$

Finally, one obtains the next order solution of the DSE,

$$(6.5) \quad \bar{G}_{\mathcal{R}}^{(m+1)}(\bar{x}) = \bar{G}_{\mathcal{R}}^{(1)}(\bar{x}) + (1 - \hat{\mathcal{R}}) \sum_{n=2}^{m+1} \alpha^n \sum_{u=1}^n \bar{x}^{-u\epsilon} \sum_{w=-n}^{\infty} \bar{g}_{u,w}^{(n)} \epsilon^w.$$

The MS-counter term is included via coefficients $g_{0,s}^{(n)}$ as in the linear case eq. (3.8). For the non-linear DSE, the MOM-counter term can not be simplified to order ϵ^0 terms like eq. (3.11). In practice, it is sufficient to include terms $\propto \epsilon^m$ if one is interested in the finite part of the Green function $G_{\mathcal{R}}^{(m)}(x)$ since every iteration potentially multiplies the result with ϵ^{-1} .

Of course, the established methods such as [12, 27, 5] are tremendously more efficient in computing the anomalous dimension. A power-series solution of the ODE eq. (6.7) to order α^{100} can be obtained in seconds while the brute-force algorithm merely reaches α^{10} symbolically after several hours. The computation of $\gamma_1(\alpha)$ is only a side effect of our algorithm, the actual result are the coefficients of $\ln(\delta(\alpha))$.

All computations, also the extraction of series coefficients in the computation of $h_t^{(n)}$ and $g_{u,w}^{(n)}$, have been done with the computer algebra system Mathematica 12.3. In practice, the computation is entirely limited by CPU time due to an explosion of series coefficients: In order to reach ϵ^0 at order α^{10} , we have to include terms up to ϵ^{10} in the intermediate steps. Further we produce pole terms up to ϵ^{-10} and contributions up to $x^{-10\epsilon}$, each $g_{t,s}^{(10)}$ requires series reversion and -multiplication. If we were to go to α^{20} , we would have to include ϵ^{20} from the start, dramatically slowing down every intermediate step.

The higher the order, the higher powers of π^2 and the more different zeta values appear. Algebraic operations with these expressions are increasingly slow. This second problem can be circumvented by working with floating point numbers, but it turns out that each iteration loses several decimal digits of precision. We computed the first orders symbolically and then continued numerically.

Thirdly, the expansions eq. (6.4) are, for large n , much harder for negative s than for small positive s due to the summation boundaries. Therefore we reach higher order for the positive s .

6.2. Results. For $s = -2$, this is the model examined in [12, 13, 11], up to a factor -2 in the definition of α , see [13, eq. (12)].

The coefficients were computed symbolically up to α^{10} for an invariant charge eq. (6.1) where $s \in \{-5, \dots, +5\}$. The results are extended up to at least α^{20} numerically with at least 30 valid decimal digits. It was verified that in all cases, the first three orders of the leading-log expansion fulfil eqs. (2.13) and (2.14).

The anomalous dimensions up to order α^8 are reported in table 6 in appendix E. Let the anomalous dimension be $\gamma_1(\alpha) = \sum_{n=0}^{\infty} c_n \alpha^n$ then the empirical values of table 6 suggest $c_0 = 0, c_1 = -1, c_2 = -(s+1), c_3 = -(1+s)(2+3s), c_4 = -(s+1)(2s+1)(7s+5)$. Further, for $s = 1$ the sequence is [33, A177384], for $s = 2$ it is [33, A064037]. The case $s = -3$ produces

$$(6.6) \quad \gamma_1(\alpha) = -\alpha + 2\alpha^2 - 14\alpha^3 + 160\alpha^4 - 2444\alpha^5 + 45792\alpha^6 - 1005480\alpha^7 + 25169760\alpha^8 \mp \dots$$

Compare this to [6, Table 1], in which $G_{\mathcal{R}}$ is inserted into both the internal edges of the primitive. Our result eq. (6.6) reproduces the purely rational part of the latter, but not the terms proportional to $\zeta(j)$.

The function $\gamma_1(\alpha) =: \gamma_1^{\text{pert}}(\alpha)$ is the perturbative solution to the differential equation 2.11,

$$(6.7) \quad -(1 + \gamma_1(\alpha)(s\alpha\partial_\alpha + 1))\gamma_1(\alpha) = \alpha.$$

This ODE has also non-perturbative solutions [9, 11] of the form

$$(6.8) \quad \gamma_1^{\text{non-pert}}(\alpha) = \alpha^\beta \exp\left(-\frac{\lambda}{\alpha}\right) \left(1 + b^{(1)}\alpha + b^{(2)}\alpha^2 + \dots\right).$$

We use the method of [9, V. A.] to determine the unknown coefficients¹. The ansatz $\gamma_1(\alpha) = \gamma_1^{\text{pert}}(\alpha) + \gamma_1^{\text{non-pert}}(\alpha)$ is inserted into eq. (6.7) and the above coefficients c_j are used for γ_1^{pert} . The

¹The author thanks Gerald Dunne for suggesting the method.

equation is then linearized in $\gamma_1^{\text{non-pert}}$. The resulting series in α has to vanish, this leads to the expressions listed in eq. (D.1), especially $\lambda(s) = 1/s, \beta(s) = -(3+2s)/s$. For $s = -2$ we reproduce [11, (25)] up to different sign conventions regarding α , mentioned above.

The coefficients c_n of the perturbative solution of the non-linear DSE eq. (6.7), grow factorially, which has been studied repeatedly [10, 11, 13, 7]. The asymptotic behaviour of c_n is dictated by the non-perturbative solution eq. (6.8), [3] (alternatively, use the methods of [7]), namely for $n \rightarrow \infty$

$$(6.9) \quad c_n \sim S(s) \cdot \frac{1}{\lambda(s)^n} \cdot \Gamma(n - \beta(s)) \left(1 + \frac{\lambda(s) \cdot b^{(1)}(s)}{(n - \beta(s) - 1)} + \frac{\lambda(s)^2 \cdot b^{(2)}(s)}{(n - \beta(s) - 1)(n - \beta(s) - 2)} + \dots \right).$$

We computed 500 series coefficients of $\gamma_1^{\text{pert}}(\alpha)$ and extracted their asymptotic behaviour using order-70 Richardson extrapolation. This produced at least 50 significant digits and confirmed the expressions $\lambda(s), \beta(s), b^{(1)}(s), b^{(2)}(s)$ and $b^{(3)}(s)$ listed in eq. (D.1). The Stokes constant $S(s)$ is reported in table 7. One recognizes [11], $S(-2) = 1/(\sqrt{\pi e})$ and also $S(-3) = 3/(\pi e^2)$, all other Stokes constants appear unfamiliar.

To visualize the asymptotic behaviour, we consider the ratio

$$(6.10) \quad \frac{c_{n+1}/\Gamma(n+1-\beta(s))}{c_n/\Gamma(n-\beta(s))} \equiv \frac{c_{n+1}}{(n + \frac{3+2s}{s})c_n} = s - b^{(1)}(s) \frac{1}{n^2} + \mathcal{O}\left(\frac{1}{n^3}\right) \quad (\text{for } s \neq 0, -1).$$

There is no $1/n$ correction to this quantity, hence it converges quickly, as shown in Figure 3 (A).

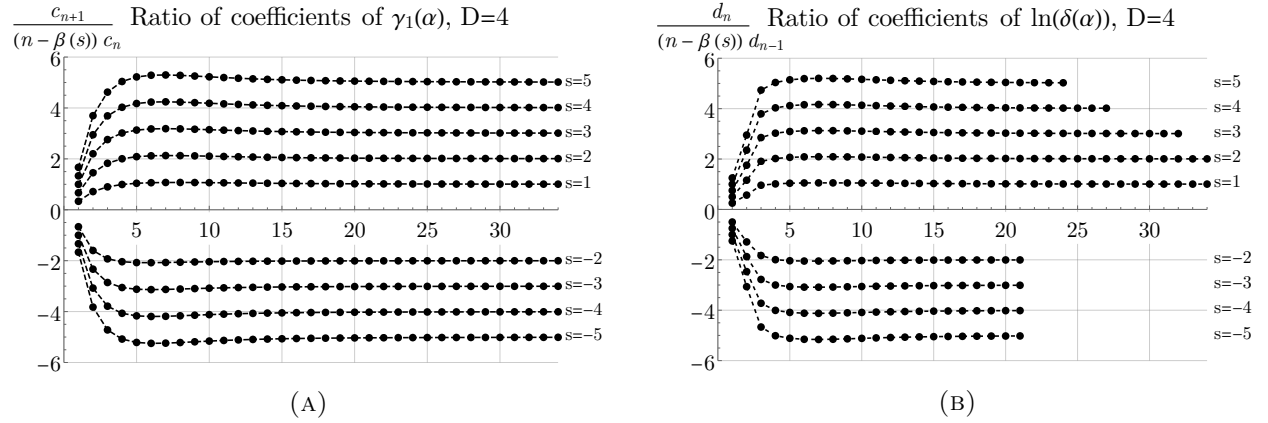


FIGURE 3. (A) Ratio of successive coefficients c_n of $\gamma_1 = \sum c_n \alpha^n$ for the physical model in $D = 4$ dimensions. The denominator $(n - \beta(s))$ is chosen to match the known asymptotics eq. (6.9). The ratio quickly converges towards the limit s , see eq. (6.10). (B) Ratio of successive coefficients d_n of $\ln(\delta) = \sum_n d_n \alpha^n$. Seemingly, it converges to the same limit s as the ratio in (A). The computation is much harder for negative s , therefore only a lower order n is available.

The shift from MOM- to MS-bar-renormalization is computed as discussed in section 2.4. The first coefficients are reported in table 8, for example, for $s = -2$ one obtains

$$\bar{\gamma}_0(\alpha) = 1 + 2\alpha - \frac{11}{2}\alpha^2 + \frac{88}{3}\alpha^3 - \left(\frac{1781}{8} + \frac{\zeta(3)}{3}\right)\alpha^4 + \left(\frac{42613}{20} + \frac{\pi^2}{150} - \frac{12\zeta(3)}{5}\right)\alpha^5 - \mathcal{O}(\alpha^6)$$

$$\ln(\bar{\delta}(\alpha)) = -2 + \frac{3}{2}\alpha - \frac{29}{6}\alpha^2 + \frac{94 - \zeta(3)}{3}\alpha^3 - \left(\frac{5573}{20} + \frac{\pi^4}{150} - \frac{7\zeta(3)}{5}\right)\alpha^4 \mp \dots$$

We write $\ln(\bar{\delta}) = \sum d_n \alpha^n$, where the coefficients d_n were computed up to order α^{10} symbolically and to at least order α^{20} numerically. As expected from eq. (2.18), the constant coefficient of $\ln(\bar{\delta})$ is $d_0 = -2$ for all s . Similarly to eq. (6.10), we examine the ratio of successive d_n , the result is shown in fig. 3 (B). We extract numerical estimates for the growth parameters in the ansatz

$$(6.11) \quad d_n \sim \tilde{S}(s) \cdot \tilde{F}(s)^n \cdot \Gamma(n - \tilde{\beta}(s)) \left(1 + \frac{\tilde{b}^{(1)}(s)}{(n - \tilde{\beta}(s) - 1)} + \dots \right)$$

by the following method: We use Richardson extrapolation[3] of orders 2,3,4 and 5 and take their mean as the estimation and the largest absolute difference between any of these as uncertainty. Experiments with the coefficients c_n of $\gamma_1(\alpha)$ show that this procedure likely overestimates the uncertainties.

s	n_{\max}	$\tilde{S}(s)/s$	$\tilde{F}(s)$	$\tilde{\beta}(s)$	$\tilde{b}^{(1)}(s)$
5	24	-0.02532 ± 0.00037	4.987 ± 0.062	-3.59 ± 0.12	-2.61 ± 0.18
4	27	-0.02709 ± 0.00019	3.993 ± 0.036	-3.74 ± 0.08	-2.79 ± 0.11
3	32	-0.02749 ± 0.00011	2.997 ± 0.017	-3.99 ± 0.04	-3.10 ± 0.06
2	38	-0.02272 ± 0.00010	1.999 ± 0.009	-4.50 ± 0.03	-3.74 ± 0.05
1	38	-0.00541 ± 0.00009	0.999 ± 0.007	-6.00 ± 0.04	-5.97 ± 0.12
-2	21	0.2080 ± 0.0018	-1.998 ± 0.012	-1.49 ± 0.05	-0.74 ± 0.08
-3	21	0.1295 ± 0.0014	-2.995 ± 0.026	-1.99 ± 0.07	-1.10 ± 0.11
-4	21	0.0882 ± 0.0011	-3.993 ± 0.040	-2.24 ± 0.09	-1.30 ± 0.14
-5	21	0.0655 ± 0.0009	-4.991 ± 0.054	-2.40 ± 0.10	-1.43 ± 0.15

TABLE 1. Numerical findings of the growth parameters of $\ln(\bar{\delta}(\alpha))$ in the $D = 4$ model section 6, according to eq. (6.11). They are consistent with table 7 and eq. (D.1). $\ln(\bar{\delta}(\alpha))$ was computed including order $\alpha^{n_{\max}}$.

The results are reported in table 1. We confirm $\tilde{S}(s) = s \cdot S(s)$, $\tilde{F}(s) = s$ and $\tilde{\beta}(s) = \beta(s) - 1$ within around 1% relative uncertainty. Unlike the above analysis of γ_1 , at this level of uncertainty our findings of “rational numbers” are to be understood as educated guesswork rather than proofs. The estimates obtained for $\tilde{b}^{(1)}(s)$ are too imprecise to deduce a formula at this point.

It turns out to be very useful to compare the coefficients of $\ln(\bar{\delta}(\alpha))$ to those of $\gamma_1(\alpha)$. To this end we compute the ratio $d_n/(s\lambda c_{n+1})$, where $s \cdot \lambda(s) = 1$ in our case. Using eq. (6.11) with table 1, we expect that $d_n/c_{n+1} \rightarrow 1$.

s	$r_1(s)$	$r_2(s)$	$r_3(s)$	$r_4(s)$	$r_5(s)$
5	1.20002 ± 0.00012	0.0003 ± 0.0019	0.005 ± 0.031	0.09 ± 0.50	1.3 ± 7.9
4	1.25000 ± 0.00001	0.0000 ± 0.0002	0.000 ± 0.003	0.01 ± 0.05	0.18 ± 0.95
3	1.33333 ± 0.00001	0.0000 ± 0.0001	0.000 ± 0.001	0.01 ± 0.01	0.00 ± 0.02
2	1.50000 ± 0.00001	0.0000 ± 0.0001	0.000 ± 0.001	0.00 ± 0.01	0.00 ± 0.01
1	2.00000 ± 0.00001	0.0000 ± 0.0001	0.000 ± 0.001	0.00 ± 0.01	0.00 ± 0.01
-2	0.50000 ± 0.00001	0.0000 ± 0.0001	0.000 ± 0.001	0.00 ± 0.01	0.00 ± 0.02
-3	0.66667 ± 0.00001	0.0000 ± 0.0002	0.000 ± 0.002	0.01 ± 0.03	0.07 ± 0.39
-4	0.75001 ± 0.00004	0.0001 ± 0.0005	0.001 ± 0.007	0.02 ± 0.09	0.20 ± 1.24
-5	0.80001 ± 0.00006	0.0002 ± 0.0009	0.002 ± 0.012	0.03 ± 0.17	0.4 ± 2.3

TABLE 2. Parameters of the ratio d_n/c_{n+1} for $D = 4$ from eq. (6.12). $r_{\geq 2}$ is consistent with zero.

As before, we use Richardson extrapolation of order 2,3,4 and 5 to determine the parameters in

$$(6.12) \quad \frac{d_n}{s\lambda c_{n+1}} \sim r(s) + r_1(s)\frac{1}{n} + r_2(s)\frac{1}{n^2} + \dots, \quad n \rightarrow \infty.$$

We find $r(s) = 1$ with uncertainty smaller 10^{-5} . The numerical results for the corrections $r_j(s)$ are reported in table 2. The relative uncertainties are much smaller than for the above parameters of eq. (6.11). They suggest the simple formula $r(s) = 1$ and $r_1(s) = (s+1)/s$. Inserting this, surprisingly, the higher order corrections $r_{j \geq 2}(s)$ seem to vanish.

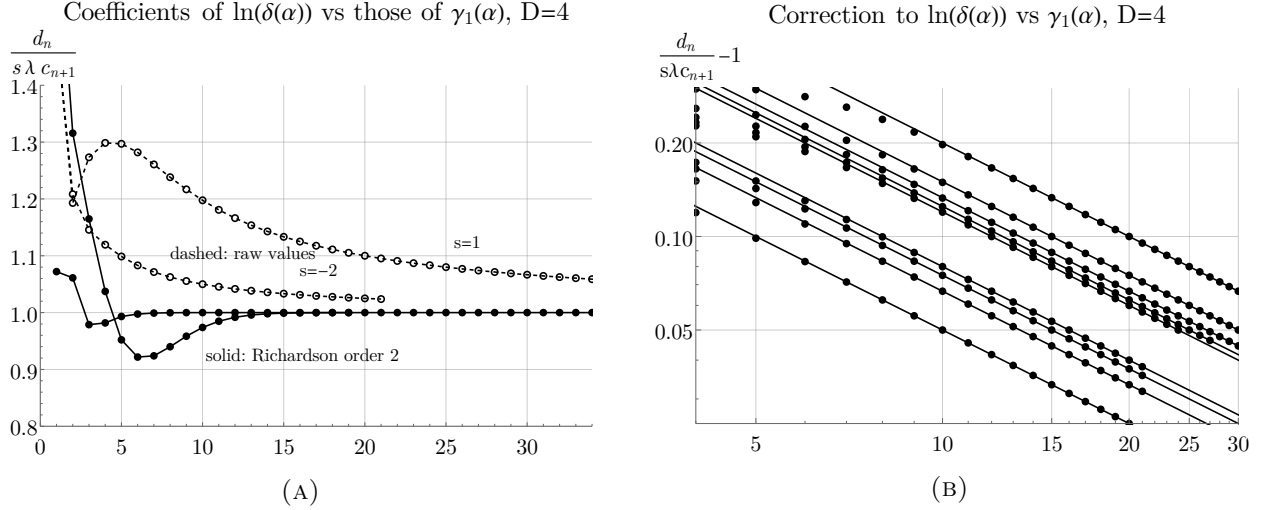


FIGURE 4. (A) Ratio of the coefficients of $\ln(\delta(\alpha)) = \sum d_n \alpha^n$ and $\gamma_1(\alpha) = \sum c_n \alpha^n$. Shown are two representative sequences, namely $s = -2$ and $s = 1$. For each of them, the dashed line indicates the raw values while the solid line is the order-2 Richardson extrapolation. The ratio d_n/c_{n+1} approaches the limit unity. (B) Correction to this ratio. The points are the values of $\frac{d_n}{c_{n+1}} - 1$ for the different s . Solid lines are the functions $\frac{s+1}{sn}$, they match the points surprisingly well even for low orders. The remaining difference falls off faster than $1/n^2$.

Together with the known behaviour of c_{n+1} , eq. (6.9) and $\beta(s) = -(3+2s)/s$, we conclude

$$(6.13) \quad d_n \sim S(s)s^{n+1}\Gamma(n - \beta(s) + 1) \left(1 + \frac{-1+3s+2s^2}{n - \beta(s)} + \frac{1+4s+4s^2-6s^3-7s^4}{(n - \beta(s))(n - \beta(s) - 1)} + \mathcal{O}\left(\frac{1}{n^3}\right) \right).$$

The subleading coefficient is consistent with the value $\tilde{b}^{(1)}(s)$ which we found in table 1.

For the higher order corrections in table 2, the uncertainties are increasing. If we nonetheless speculate that their vanishing is a general pattern, then we obtain

$$(6.14) \quad d_n = \left(1 + \frac{s+1}{sn}\right) \cdot c_{n+1} + e_n.$$

The numerical values suggest that the remainder e_n falls off factorially, see fig. 5 (A). Using the ring of factorially divergent power series[10], this asymptotic statement can be translated to a relation between the corresponding generating functions²:

$$(6.15) \quad \ln(\bar{\delta}(\alpha)) = \frac{\gamma_1(\alpha)}{\alpha} + \frac{s+1}{s} \int \frac{d\alpha}{\alpha} \frac{\gamma_1(\alpha)}{\alpha} + f(\alpha), \quad s \neq 0.$$

²The author thanks Michael Borinsky for pointing this out

Figure 5 (B) shows the coefficients of the function $f(\alpha) = \sum_{n=1}^{\infty} f_n \alpha^n$, they grow exponentially. This indicates that $f(\alpha)$ is an analytic function, given by a convergent power series around $\alpha = 0$. The growth rate is reported in table 8. The coefficients of the function $f(\alpha)$ contain zeta values, which appear in $\ln(\hat{\delta}(\alpha))$ but not in $\gamma_1(\alpha)$. We have not succeeded in finding a closed formula.

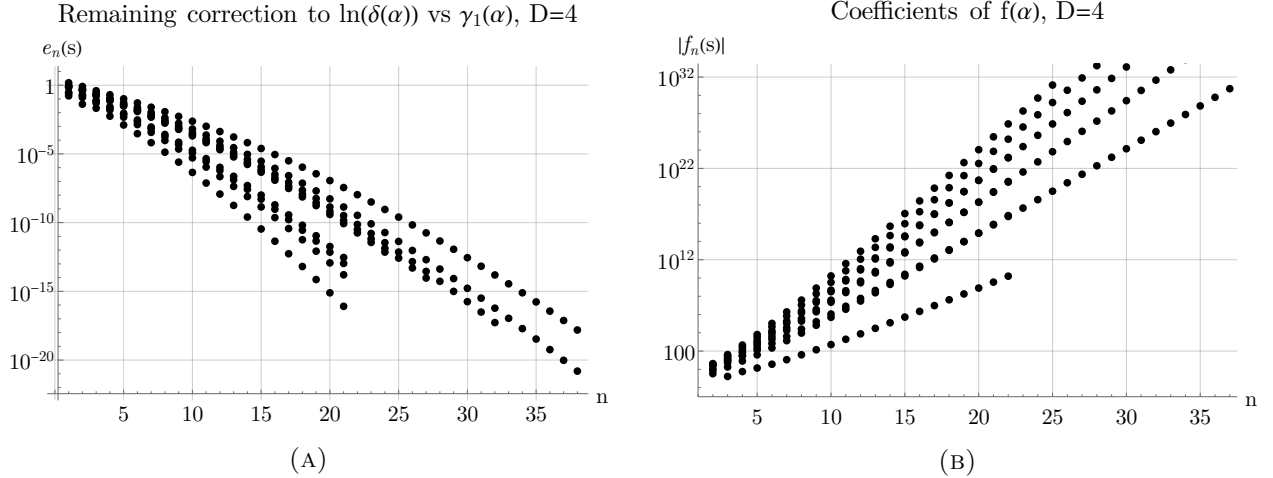


FIGURE 5. (A) Remainder coefficients e_n from eq. (6.14), for the different values of s . This is a logarithmic plot, therefore they decay faster than exponentially. (B) Coefficients of the function $f(\alpha)$ in eq. (6.15). The data points overlap for different s . The coefficients grow exponentially, which suggests that $f(\alpha)$ is an analytic function.

7. NON-LINEAR DSE IN $D = 6$

Following the procedure of section 6.1, we also evaluate the 6-dimensional model of section 4 for various powers $s \in \{-5, \dots, +5\}$ in the invariant charge eq. (6.1).

The leading-log functions H_1, H_2, H_3 are as expected from eq. (2.13). The anomalous dimension $\gamma_1(\alpha)$ contains only rational coefficients for all values of s . Up to the computed symbolic precision α^{12} , they fulfil the ODE eq. (2.11), which here takes the form

$$(7.1) \quad (3 + \gamma_1(s\alpha\partial_\alpha + 1))(2 + \gamma_1(s\alpha\partial_\alpha + 1))(1 + \gamma_1(s\alpha\partial_\alpha + 1))\gamma_1 = \alpha.$$

The perturbative solution $\gamma_1^{\text{pert}}(\alpha) = \sum_{j=0}^{\infty} c_j \alpha^j$ can be computed to high order from this ODE, the first coefficients are

$$c_1 = \frac{1}{6}, \quad c_2 = -\frac{11(s+1)}{216}, \quad c_3 = \frac{(s+1)(206+291s)}{7776}, \quad c_4 = -\frac{(s+1)(4711+14887s+11326s^2)}{279936}.$$

We use these coefficients, insert the non-perturbative ansatz eq. (6.8) into eq. (7.1), linearize, and solve for the parameters $\beta, \lambda, b^{(1)}, b^{(2)}, b^{(3)}$. Equation (7.1) is of third order, unlike in the case $D = 4$, we find three linearly independent solutions eq. (D.2). In the ansatz eq. (6.8), the solution with smallest absolute λ is dominant, this is the first entry of the vectors eq. (D.2).

With these parameters, the series coefficients c_n of the perturbative solution grow according to eq. (6.9). We have confirmed this behaviour numerically from the first 500 coefficients c_n for $s \in \{-5, \dots, +5\}$. The Stokes constant $S(s)$ is reported in table 9, we reproduce the value [9, (15)] for $s = -2$. Like eq. (6.10), the ratio of successive coefficients $c_{n+1}/((n - \beta_1(s))c_n)$ is constant up to quadratic corrections.

The power series coefficients of the shift $\ln(\hat{\delta})$ have been computed symbolically up to order α^{10} , the leading ones are reported in table 10. The numerical computation extends further, depending on

s . The ratio of successive coefficients, with the same normalization as for γ_1 , is shown in fig. 6(A). The plot suggests that c_n grow at a similar rate as d_n .

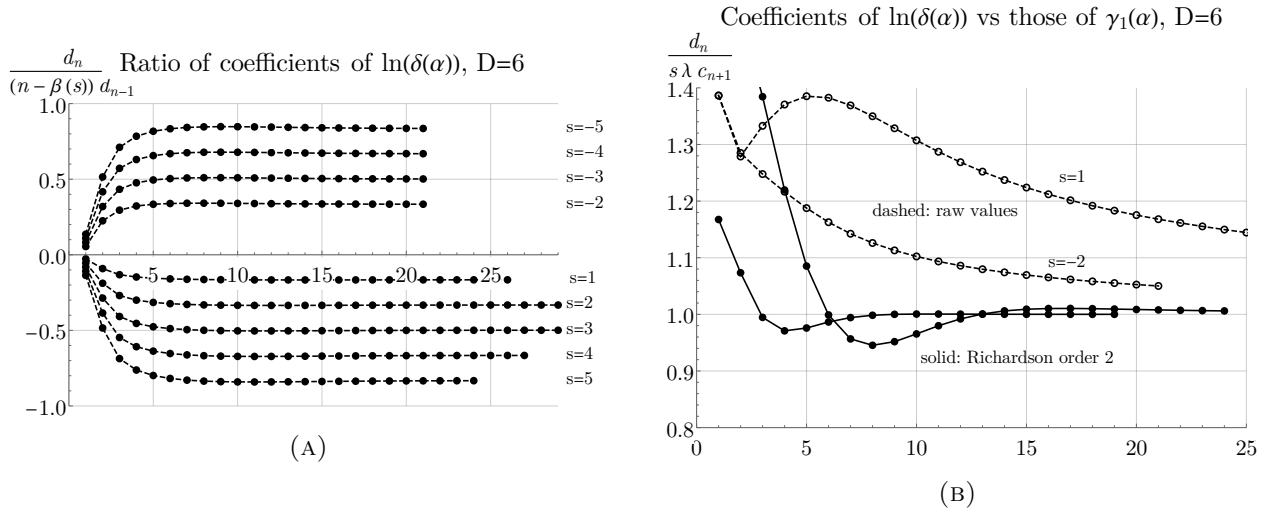


FIGURE 6. (A) Ratio of successive coefficients d_n of $\ln(\delta(\alpha))$, divided by the assumed leading asymptotic behaviour from eq. (D.2), for $D = 6$. This quantity quickly approaches the limit $-s/6$. (B) Ratio between the coefficients d_n of $\ln(\delta(\alpha))$ and the coefficients c_{n+1} of $\gamma_1(\alpha)$. Compared to fig. 4 (A), the Richardson extrapolation converges slower, indicating a significant $1/n^2$ -correction, see table 4.

As explained in section 6.2, we extracted numerical estimates of the parameters in eq. (6.11). They are given in table 3 and are consistent with $\tilde{S}(s) = s \cdot S(s)$, $\tilde{F}(s) = -s/6$ and $\tilde{\beta}(s) = \beta_1(s) - 1$. Once more, the relative uncertainty of about 1% of these values is too large to rigorously identify the rational values.

s	n_{\max}	$10^6 \cdot \tilde{S}(s)/s$	$\tilde{F}(s)$	$\tilde{\beta}(s)$
5	24	-50.1 ± 4.5	-0.833 ± 0.018	-7.00 ± 0.37
4	27	-34.5 ± 2.4	-0.666 ± 0.012	-7.25 ± 0.23
3	29	-16.6 ± 1.2	-0.500 ± 0.007	-7.72 ± 0.19
2	29	-2.97 ± 0.28	-0.333 ± 0.006	-8.68 ± 0.26
1	26	-0.0054 ± 0.0015	-0.167 ± 0.006	-11.64 ± 0.75
-2	21	87900 ± 1600	0.333 ± 0.005	-2.92 ± 0.12
-3	21	18000 ± 560	0.500 ± 0.009	-3.90 ± 0.21
-4	21	6690 ± 290	0.666 ± 0.013	-4.39 ± 0.26
-5	21	3410 ± 180	0.833 ± 0.018	-4.69 ± 0.29

TABLE 3. Numerical findings of the growth parameters of $\ln(\bar{\delta}(\alpha))$ in the $D = 6$ model section 7, according to eq. (6.11). They are consistent with table 9 and eq. (D.2).

The ratio $d_n/(s\lambda c_{n+1}) = d_n/(-6c_{n+1})$ is depicted in fig. 6 (B) for two values of s . The asymptotic parameters, according to eq. (6.12), are given in table 4. Unlike for $D = 4$, this ratio does not converge particularly quickly. A fit suggests that $r_1(s) = (2.12 + 2.15s)/s$, but the uncertainties are too large to identify these numbers as rational. This is reflected by the large absolute values we

s	$r(s)$	$r_1(s)$	$r_2(s)$
5	1.0010 ± 0.0017	2.573 ± 0.072	-6.91 ± 0.84
4	1.0007 ± 0.0019	2.685 ± 0.072	-7.3 ± 1.4
3	1.0007 ± 0.0024	2.863 ± 0.078	-8.4 ± 1.8
2	1.0010 ± 0.0026	3.21 ± 0.11	-11.2 ± 1.8
1	1.0032 ± 0.0048	4.22 ± 0.23	-22.3 ± 1.3
-2	1.0000 ± 0.0002	1.083 ± 0.003	-1.10 ± 0.34
-3	1.0002 ± 0.0004	1.441 ± 0.012	-1.80 ± 0.07
-4	1.0003 ± 0.0007	1.619 ± 0.018	-2.33 ± 0.16
-5	1.0004 ± 0.0008	1.726 ± 0.022	-2.71 ± 0.22

TABLE 4. Parameters of the ratio $d_n/(-6c_{n+1})$ for $D = 6$ from eq. (6.12).

obtain for the $1/n^2$ -correction $r_2(s)$, see table 4. In $D = 4$, this correction vanished and therefore allowed us to extract $r_1(s)$ precisely.

All in all, we can not clearly identify the subleading corrections of d_n in the $D = 6$ model, but at least the findings suggest that the leading growth coincides with the one of c_{n+1} , that is

$$(7.2) \quad d_n \sim S(s)s \left(-\frac{s}{6}\right)^n \Gamma\left(n + 1 + \frac{35 + 29s}{6s}\right).$$

8. NON-LINEAR TOY MODEL

We solved the DSE for $s \in \{-5, \dots, +4\}$ symbolically to order α^{16} . The leading-log functions H_1, H_2 and H_3 agree with the general formula eq. (2.13) of [28] for the appropriate choice $g_1 = 1, g_2 = 0, g_3 = \pi^2/2$ and for all choices of s . Especially, for $s = -2$, we confirm H_1 from [31, Cor. 3.6.4] and $H_2 = H_4 = H_6 = 0$.

The symbolic results for the anomalous dimension fulfil eq. (2.11),

$$(8.1) \quad -\frac{\sin(u)}{u} \Big|_{u \rightarrow -\gamma_1(s\alpha\partial_\alpha + 1)} \gamma_1 = \alpha.$$

Unlike eqs. (6.7) and (7.1), the ODE eq. (8.1) of the toy model is of infinite order. This is in interesting contrast to the comparatively simple integral kernel coefficients eq. (B.4) of the toy model.

We computed a symbolic perturbative power series solution $\gamma_1(\alpha) = \sum c_n \alpha^n$ of eq. (8.1) to order 450 and extracted the asymptotic behaviour. The result has the form eq. (6.9) for n odd. We find $\beta(s) = -(2 + s)/s$, numerical values of the constants $S(s), b^{(1)}(s)$ and $b^{(2)}(s)$ are given in table 11. We did not recognize these numbers apart from the Stokes constant $S(-2) = 2/\pi$.

By eq. (2.18), the shift $\ln(\delta) = \sum d_n \alpha^n$ does not have a constant term in the toy model. The first coefficients for the shift are reported in table 12, while table 5 contains the numerical estimates for the growth parameters.

The toy model has the property that both c_n and d_n vanish for even n . This is problematic for two reasons: Firstly, although we computed numerically the order α^{23} , we only get 12 non-vanishing coefficients of $\ln(\delta)$. Secondly, we can not compute the ratio d_n/c_{n+1} and therefore not use the trick which allowed us to extract the behaviour of d_n in the $D = 4$ physical model section 6.

To visualize the coefficients d_n of $\ln(\delta(\alpha))$, we consider the following two ratios for odd n :

$$(8.2) \quad R^{(\delta)} := \sqrt{\frac{d_{n+2}}{(n - \beta(s) + 1)(n - \beta(s) + 2)d_n}}, \quad R^{(\delta/\gamma)} := \frac{d_n}{s \cdot (n - \beta(s) + 1)c_n}.$$

s	n_{\max}	$\tilde{S}(s)/s$	$\tilde{F}(s)$	$\tilde{\beta}(s)$
4	23	-0.389 ± 0.010	3.985 ± 0.081	-2.50 ± 0.21
3	23	-0.485 ± 0.015	2.988 ± 0.068	-2.68 ± 0.24
2	23	-0.612 ± 0.023	1.991 ± 0.059	-3.02 ± 0.31
1	23	-0.572 ± 0.037	0.996 ± 0.056	-4.09 ± 0.56
-2	23	0.6382 ± 0.0067	1.997 ± 0.012	-0.991 ± 0.050
-3	23	0.5275 ± 0.0076	2.994 ± 0.024	-1.322 ± 0.071
-4	23	0.4202 ± 0.0069	3.991 ± 0.037	-1.488 ± 0.082
-5	23	0.3443 ± 0.0060	4.988 ± 0.051	-1.588 ± 0.088

TABLE 5. Numerical findings of the growth parameters of $\ln(\bar{\delta}(\alpha))$ in the toy model, according to eq. (6.11). $\tilde{S}(s)$ is consistent with table 11.

Figure 7 (A) shows that $R^{(\delta)}$ approaches the limit $|s|$, which suggests that d_n scale asymptotically $\sim s^n \Gamma(n - \beta(s) + 1)$, with (approximately) the same $\beta(s)$ as the coefficients c_n of $\gamma_1(\alpha)$. The quantity $R^{(\delta/\gamma)}$ allows to fix the Stokes constant, it is shown in fig. 7 (B). The limit of $R^{(\delta/\gamma)}$ is 1.00 ± 0.02 , suggesting that the Stokes constant agrees with the one of $\gamma_1(\alpha)$. In table 5, the direct estimates of the asymptotic growth are reported. All in all, it seems that the coefficients of $\ln(\delta(\alpha))$ grow factorially according to

$$(8.3) \quad d_n \sim S(s) s^{n+1} \Gamma(n + (2 + 2s)/s).$$

We did not try to determine subleading corrections.

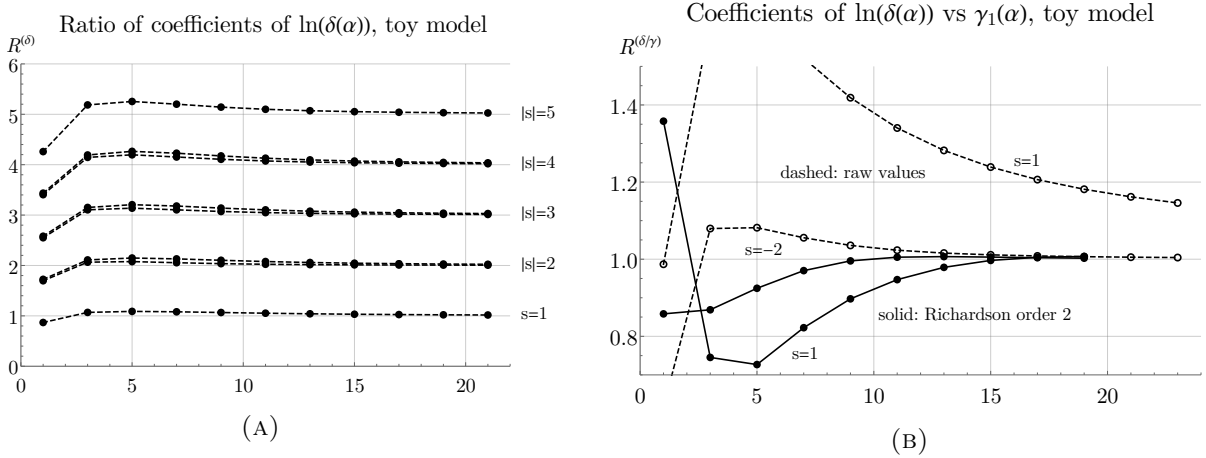


FIGURE 7. (A) Ratio eq. (8.2) of successive coefficients of $\ln(\delta(\alpha))$. The ratio visibly approaches $|s|$, Richardson extrapolation (not shown) confirms this. (B) Ratio $R^{(\delta/\gamma)}$ between coefficients of $\ln(\delta(\alpha))$ and $\gamma_1(\alpha)$ and its order-2-Richardson extrapolation. The limit seems to be unity, but knowing only 12 terms the uncertainty is large. Compare the first 12 terms of fig. 4 (A).

The MS counter term has been computed symbolically up to order α^{16} . For the choice $s = -2$, and only there, it empirically reproduces the leading log order eq. (2.13) of the Green function:

$$\hat{Z}(\alpha, \epsilon) = 1 + \sum_{n=1}^{16} 2C_{n-1} \left(\frac{\alpha}{2\epsilon}\right)^n + \mathcal{O}(\alpha^{17}) = \sqrt{1 - 2\alpha \frac{1}{\epsilon}} + \mathcal{O}(\alpha^{17}) = H_1\left(\alpha \frac{1}{\epsilon}\right) + \mathcal{O}(\alpha^{17}).$$

We take this as a curiosity and motivation for future systematic examinations.

9. CONCLUSION

We have analyzed propagator-type Dyson-Schwinger equations with three different kernels in minimal subtraction. For various relevant quantities, we have computed their series coefficients symbolically and identified the coefficients' algebraic formulas. In all cases where there is an overlap, our results agree with the ones reported in earlier literature. The key outcomes of the present work are:

- (1) The all-order Green functions in MS and MS-bar agree, in the limit $\epsilon \rightarrow 0$, with the Green function in kinematic renormalization if a suitable kinematic renormalization point $\delta(\alpha) \cdot \mu$ is chosen, where μ is the mass scale of dimensional regularization.
- (2) In the linear examples, the factors $\delta(\alpha)$ between the renormalization points have been deduced in closed form as $\delta(\alpha) = \gamma_0^{1/\gamma_1}$, see eqs. (3.15), (4.1) and (5.2). The result is finite in perturbation theory and proportional to $\sqrt{\partial_\alpha \gamma_1(\alpha)}$.
- (3) For non-linear DSEs, series coefficients for $\gamma_1(\alpha)$ and $\ln(\delta(\alpha))$ have been computed for ten different exponents s in the invariant charge $Q = (G_{\mathcal{R}})^s$. The results are highly regular in s . The first symbolic coefficients of $\ln(\delta)$ are collected in appendix E.
- (4) The coefficients d_n of $\ln(\delta(\alpha))$ seem to grow factorially. In all cases, we find $d_n \sim S \cdot s \cdot \lambda^{-n} \cdot \Gamma(n - \beta + 1)$, where S, λ and β are the growth parameters of the corresponding anomalous dimension γ_1 eqs. (6.13), (7.2) and (8.3). This suggests that $\delta(\alpha)$ receives non-perturbative contributions in the same way as $\gamma_1(\alpha)$ does [11, 9].
- (5) For the $D = 4$ physical model, the ratio d_n/c_{n+1} between coefficients of $\ln(\delta(\alpha))$ and γ_1 is extremely well behaved and allows to deduce two subleading corrections to the growth of d_n eq. (6.13). If this pattern continues, then the non-perturbative part of $\ln(\delta(\alpha))$ can be computed from $\gamma_1(\alpha)$, eq. (6.15).
- (6) In the linear examples, the renormalization counter terms \hat{Z} in MS-renormalization have been found in closed form. The function $Z(\alpha, \epsilon)$ lies in $[0, 1]$ if α and ϵ share the same sign and it vanishes smoothly in the limit $\epsilon \rightarrow 0$.
- (7) For linear DSEs, the MOM counter term encodes the shift $\delta(\alpha)$ of the renormalization point between MOM and MS via eq. (3.22). If the MOM-renormalized Green function is known for $\epsilon \neq 0$ then this shift can be computed exactly from eq. (3.23).

All examples indicate that there is a significant offset factor $\delta(\alpha)$ between the mass scale μ of MS-renormalization and the corresponding kinematic renormalization point. By eq. (2.18), the offset does not vanish in the limit of vanishing coupling. Consequently one should be careful not to confuse the mass scale μ of MS-renormalization with a kinematic renormalization point, even in the most well-behaved cases.

For the linear DSEs, we have found an explicit map $\gamma_1(\alpha) \mapsto \ln(\delta(\alpha))$ in eqs. (3.15), (4.1) and (5.2). For the non-linear DSEs, this connection is not quite so simple. Intuitively, the identical asymptotic growth hints at the possibility to find an explicit map as well. Indeed, for the $D = 4$ case, assuming that our empirical findings hold to all orders, eq. (6.15) reproduces the factorial growth of d_n and therefore the non-perturbative behaviour. The remainder function $f(\alpha)$ in this case contains all the zeta values which appear in $\ln(\delta(\alpha))$ but not in $\gamma_1(\alpha)$.

APPENDIX A. MELLIN TRANSFORMS

The Mellin transform is by definition the value of the primitive integral where one of the propagators is raised to a power $1 + \rho$, evaluated at unity external momentum. Factors of 4π from the Fourier transform are implicitly absorbed into the mass scale in the main text, therefore they are

left out from the Mellin transform. For the 4-dimensional resp. 6-dimensional propagator,

$$M(\rho) = \int \frac{d^4 k (k^2)^{-\rho}}{(k+q)^2 k^2} \Big|_{q^2=1} = \frac{1}{\rho(1-\rho)}, \quad M(\rho) = \int \frac{d^6 k (k^2)^{-\rho}}{(k+q)^2 k^2} \Big|_{q^2=1} = -\frac{1}{\rho(1-\rho)(2-\rho)(3-\rho)}.$$

The Mellin transform in the toy model is

$$M(\rho) = \int_0^\infty \frac{dy y^{-\rho}}{x+y} \Big|_{x=1} = \frac{\pi}{\sin(\pi\rho)}.$$

APPENDIX B. SERIES EXPANSION OF THE PRIMITIVE GRAPHS

We are interested in the series expansion in ϵ of the integral

$$\begin{aligned} I_D^{(k)}(q) &:= \int \frac{d^D p}{(2\pi)^D} \frac{1}{(p+q)^2 (p^2)^{1+k\epsilon}} \\ &= (4\pi)^{-\frac{D}{2}} (q^2)^{\frac{D}{2}-2-k\epsilon} \frac{\Gamma(-\frac{D}{2}+2+k\epsilon) \Gamma(\frac{D}{2}-1) \Gamma(\frac{D}{2}-1-k\epsilon)}{\Gamma(1+k\epsilon) \Gamma(D-2-k\epsilon)} \\ &=: (4\pi)^{-\frac{D}{2}} (q^2)^{\frac{D}{2}-2-k\epsilon} e^{-\gamma_E \epsilon} \sum_n f_n^{(k)} \epsilon^n. \end{aligned}$$

The factors of q^2 must not be expanded into logarithms, in order to be integrated in the next iteration. Furthermore, we do not expand the (4π) and factor out $e^{-\gamma_E \epsilon}$ because both can conveniently be absorbed into the momentum. It remains to expand the gamma functions using

$$\Gamma(x+1) = x\Gamma(x), \quad \Gamma(1+\epsilon) = \exp\left(-\gamma_E \epsilon + \sum_{m=2}^{\infty} \frac{(-\epsilon)^m}{m} \zeta(m)\right).$$

In $D = 4 - 2\epsilon$ dimensions one obtains

$$\Gamma := \frac{\Gamma((k+1)\epsilon)\Gamma(1-(k+1)\epsilon)\Gamma(1-\epsilon)}{\Gamma(1+k\epsilon)\Gamma(2-(k+2)\epsilon)} = \frac{1}{(k+1)(1-(k+2)\epsilon)\epsilon} \exp\left(-\gamma_E \epsilon + \sum_{m=2}^{\infty} T_m^{(k)} \epsilon^m\right),$$

$$(B.1) \quad \text{where} \quad T_m^{(k)} := (m-1)!((-1)^m(k+1)^m + (k+1)^m + 1 - (-k)^m - (k+2)^m) \zeta(m).$$

Expanding the prefactor in a geometric series and leaving out $e^{-\gamma_E \epsilon}$,

$$(B.2) \quad f_n^{(k)} = \sum_{t=-1}^n \frac{(k+2)^{t+1}}{k+1} \frac{1}{(n-t)!} \sum_{m=0}^{n-t} B_{n-t,m} \left(0, T_2^{(k)}, T_3^{(k)}, \dots, T_{n-t+1-m}^{(k)}\right).$$

Here $B_{n,k}$ are incomplete Bell polynomials [4] [16, p 134]. For $D = 6 - 2\epsilon$ dimensions, observe

$$\frac{\Gamma(-1+(k+1)\epsilon)\Gamma(2-\epsilon)\Gamma(2-(k+1)\epsilon)}{\Gamma(1+k\epsilon)\Gamma(4-(k+2)\epsilon)} = \frac{\epsilon-1}{(3-(k+2)\epsilon)(2-(k+2)\epsilon)} \cdot \Gamma.$$

The gamma functions on the right hand side are the same as in $D = 4 - 2\epsilon$, consequently their series expansion is again given by the polynomials $T_m^{(k)}$ from eq. (B.1).

(B.3)

$$f_n^{(k)} = \sum_{t=-1}^n \left(-k+1 + \frac{k}{2^{t+1}} - \frac{k-1}{3^{t+2}}\right) \frac{(k+2)^t}{2(k+1)(n-t)!} \sum_{m=0}^{n-t} B_{n-t,m} \left(0, T_2^{(k)}, \dots, T_{n-t+1-m}^{(k)}\right).$$

In the toy model, the relevant integral and its series expansion are

$$\int_0^{\infty} \frac{dy y^{-(k+1)\epsilon}}{1+y} = \frac{\pi}{\sin(\pi(k+1)\epsilon)} = \Gamma((k+1)\epsilon)\Gamma(1-(k+1)\epsilon) =: \sum_{n=-1}^{\infty} f_n^{(k)} \epsilon^n.$$

The Bernoulli numbers B_n vanish when $n > 1$ is odd, therefore we can write

$$(B.4) \quad f_n^{(k)} := \frac{1}{(k+1)} \sum_{m=0}^{n+1} \frac{1}{(n+1)!} B_{n+1,m} \left(0, T_2^{(k)}, \dots, T_{n+2-m}^{(k)}\right), \quad T_n^{(k)} := \left(2\pi(k+1)\right)^n \frac{|B_n|}{n}.$$

APPENDIX C. KINEMATIC COUNTER TERM OF THE LINEAR TOY MODEL

These are the first coefficients of eq. (5.3) for the toy model. Define $A := \alpha^2 \pi^2$.

$$\begin{aligned} z_1 &= \frac{\alpha\pi^2(4+A)}{24(1-A)^{\frac{3}{2}}}, & z_2 &= \frac{\alpha^2\pi^4(3+2A)}{16(1-A)^3}, & z_3 &= \frac{\alpha\pi^4(112+2240A+2919A^2+254A^3)}{5760(1-A)^{\frac{9}{2}}}, \\ z_4 &= \frac{\alpha^2\pi^6(36+515A+900A^2+240A^3+4A^4)}{384(1-A)^6}, \\ z_5 &= \frac{\alpha\pi^6(1984+522152A+6074220A^2+12882535A^3+6095260A^4+511956A^5+1768A^6)}{967680(1-A)^{\frac{15}{2}}}, \\ z_6 &= \frac{\alpha^2\pi^8(471+42058A+428661A^2+1041030A^3+715270A^4+129414A^5+4092A^6+4A^7)}{11520(1-A)^9}. \end{aligned}$$

All explicitly determined functions $z_n(\alpha)$ for $n > 0$ behave qualitatively similar: They diverge like $(1-A)^{-\frac{3}{2}n}$ as $\alpha\pi \rightarrow 1$ and are positive for $0 \leq \alpha < \frac{1}{\pi}$. In this interval, they give rise to a finite Z -factor. The other coefficients in eq. (5.3) are

$$\begin{aligned} z'_1 &= \frac{1}{\epsilon} + \frac{\pi^2}{6}\epsilon + \frac{7\pi^4}{360}\epsilon^3 + \dots = -\frac{1}{\epsilon} \sum_{n=0}^{\infty} \frac{(-1)^n(4^n-2)B_{2n}}{(2n)!} \pi^{2n} \epsilon^{2n} = \pi \left(\cot\left(\frac{\pi}{2}\epsilon\right) - \cot(\pi\epsilon) \right), \\ z'_2 &= \frac{\pi^2}{4} \frac{1}{\cos^2\left(\frac{\pi}{2}\epsilon\right) \cos(\pi\epsilon)}, & z'_3 &= \frac{\pi^3}{12} \frac{1-2\cos(2\pi\epsilon)+2\cos(\pi\epsilon)}{(2\cos(\pi\epsilon)+3\cos(3\pi\epsilon)) \sin\left(\frac{\pi}{2}\epsilon\right) \cos^3\left(\frac{\pi}{2}\epsilon\right)}, \\ z'_4 &= -\frac{\pi^4}{4} \frac{\cos(\pi\epsilon)+2\sin^2(\pi\epsilon)}{\cos^4(\pi\epsilon)(\cos(\pi\epsilon)-4\cos^2(\pi\epsilon)\cos(2\pi\epsilon)+\cos(3\pi\epsilon))}. \end{aligned}$$

The functions $z'_n(\epsilon)$ are positive for small positive ϵ . They change sign at their poles but probably, there are other continuations of the series expansion around $\epsilon = 0$ beyond the poles, which stay positive. For example

$$z'_2(\epsilon) = \frac{\pi^2}{2} \left(\frac{1}{\sin^2(\pi\epsilon)} - \frac{|\cot(\pi\epsilon) - \cot\left(\frac{\pi}{2}\epsilon\right)|^3}{|\cot(\pi\epsilon)|} \right)$$

is always positive and reduces to the above form of z'_2 for $|\epsilon| < 0.5$. If this holds for all z'_n then $Z(\alpha, \epsilon) \in [0, 1]$, which allows to interpret Z as a probability.

APPENDIX D. ASYMPTOTIC GROWTH OF THE ANOMALOUS DIMENSION

For the 4-dimensional physical model, the ansatz eq. (6.8) delivers the growth parameters

$$(D.1) \quad \lambda = \frac{1}{s}, \quad \beta(s) = -\frac{3+2s}{s}, \quad b^{(1)}(s) = -\frac{1+4s+3s^2}{s}, \quad b^{(2)}(s) = \frac{1+6s+8s^2-2s^3-5s^4}{2s^2}$$

$$b^{(3)}(s) = \frac{-1-6s-s^2+24s^3-25s^4-126s^5-81s^6}{6s^3}.$$

They match [11, (14)] for $s = -2$. For the 6-dimensional physical model, there are three solutions:

$$(D.2) \quad \vec{\lambda}(s) = \left(-\frac{6}{s}, -\frac{12}{s}, -\frac{18}{s} \right), \quad \vec{\beta}(s) = \left(-\frac{35+29s}{6s}, -\frac{5+2s}{3s}, -\frac{15+13s}{2s} \right)$$

$$\vec{b}^{(1)}(s) = \left(\frac{-275-267s+8s^2}{216s}, \frac{265+624s+359s^2}{108s}, \frac{85+241s+156s^2}{72s} \right)$$

$$\vec{b}^{(2)}(s) = \left(\frac{75625+83790s-101849s^2-177828s^3-67814s^4}{93312s^2}, \frac{70225+339690s+602764s^2+465258s^3+131959s^4}{23328s^2}, \frac{7225+37950s+69779s^2+51628s^3+12574s^4}{10368s^2} \right)$$

$$\vec{b}^{(3)}(s) = \left(\frac{-20796875-8551125s+107422197s^2+206297091s^3+177713418s^4+90251478s^5+23658704s^6}{60466176s^3}, \frac{18609625+138592350s+424432473s^2+687305592s^3+624311121s^4+303609366s^5+62154089s^6}{7558272s^3}, \frac{614125+4453575s+12499453s^2+16989843s^3+11830354s^4+4259034s^5+758520s^6}{2239488s^3} \right)$$

Including order $1/n^3$, the large-order growth of c_n is determined entirely by the first component of these vectors. In order to match [9, eqs. (41)-(43)], $b^{(1)}$ has to be multiplied with 3, $b^{(2)}$ with 9 and $b^{(3)}$ with 27. Parameters for the toy model are given in table 11.

APPENDIX E. TABLES

s	$\gamma_1(\alpha)$
5	$-\alpha - 6\alpha^2 - 102\alpha^3 - 2640\alpha^4 - 87804\alpha^5 - 3483072\alpha^6 - 158329512\alpha^7 - 8050087584\alpha^8$
4	$-\alpha - 5\alpha^2 - 70\alpha^3 - 1485\alpha^4 - 40370\alpha^5 - 1306370\alpha^6 - 48365100\alpha^7 - 2000065725\alpha^8$
3	$-\alpha - 4\alpha^2 - 44\alpha^3 - 728\alpha^4 - 15368\alpha^5 - 384960\alpha^6 - 11004672\alpha^7 - 350628096\alpha^8$
2	$-\alpha - 3\alpha^2 - 24\alpha^3 - 285\alpha^4 - 4284\alpha^5 - 75978\alpha^6 - 1530720\alpha^7 - 34237485\alpha^8$
1	$-\alpha - 2\alpha^2 - 10\alpha^3 - 72\alpha^4 - 644\alpha^5 - 6704\alpha^6 - 78408\alpha^7 - 1008480\alpha^8$
0	$-\alpha - \alpha^2 - 2\alpha^3 - 5\alpha^4 - 14\alpha^5 - 42\alpha^6 - 132\alpha^7 - 429\alpha^8$
-1	$-\alpha$
-2	$-\alpha + \alpha^2 - 4\alpha^3 + 27\alpha^4 - 248\alpha^5 + 2830\alpha^6 - 38232\alpha^7 + 593859\alpha^8$
-3	$-\alpha + 2\alpha^2 - 14\alpha^3 + 160\alpha^4 - 2444\alpha^5 + 45792\alpha^6 - 1005480\alpha^7 + 25169760\alpha^8$
-4	$-\alpha + 3\alpha^2 - 30\alpha^3 + 483\alpha^4 - 10314\alpha^5 + 268686\alpha^6 - 8167068\alpha^7 + 281975715\alpha^8$
-5	$-\alpha + 4\alpha^2 - 52\alpha^3 + 1080\alpha^4 - 29624\alpha^5 + 988288\alpha^6 - 38377152\alpha^7 + 1689250176\alpha^8$

TABLE 6. Non-linear DSE in $D = 4$ dimensions, see section 6.2. Series expansion of the anomalous dimension as a function of the renormalized coupling α up to order α^8 for various powers s of the invariant charge $Q = (G_{\mathcal{R}})^s$. Only insertions into a single internal edge were performed in all cases.

s	$S(s)$
5	-0.025 296 711 447 842 155 554 062 589 810 922 604 262 477 942 805 771
4	-0.027 093 755 285 804 302 538 145 834 438 779 321 901 953 254 099 492
3	-0.027 514 268 695 235 967 509 951 466 619 196 206 136 028 416 088 749
2	-0.022 754 314 527 304 604 570 864 961 094 569 471 756 231 077 114 904
1	-0.005 428 317 993 266 202 636 748 034 138 132 075 286 101 589 263 688 3
-2	0.207 553 748 710 297 351 670 134 124 720 668 682 684 453 514 969 63
-3	0.129 235 675 811 091 778 715 229 366 859 663 994 914 292 887 084 30
-4	0.087 977 369 959 821 254 076 048 394 021 324 447 743 442 962 588 612
-5	0.065 314 016 354 658 749 144 010 387 750 377 100 215 558 556 707 446

TABLE 7. First 50 digits of the Stokes constant $S(s)$ for the non-linear DSE in $D = 4$, see eq. (6.9). One finds $S(-2) = (\sqrt{\pi}e)^{-1}$ and $S(-3) = 3(\sqrt{\pi}e)^{-2}$

s	$\ln(\bar{\delta}(\alpha))$	f_{n+1}/f_n
5	$-2 - 9\alpha + (-139 + 14\zeta(3))\alpha^2 + \left(-3464 - \frac{7\pi^4}{12} + 233\zeta(3)\right)\alpha^3$	30.22 ± 0.09
4	$-2 - \frac{15}{2}\alpha + \left(-\frac{575}{6} + 10\zeta(3)\right)\alpha^2 + \left(-\frac{23525}{12} - \frac{\pi^4}{3} + \frac{410}{3}\zeta(3)\right)\alpha^3$	25.09 ± 0.06
3	$-2 - 6\alpha + \left(-\frac{182}{3} + \frac{20}{3}\zeta(3)\right)\alpha^2 + \left(-\frac{2911}{3} - \frac{\pi^4}{6} + \frac{214}{3}\zeta(3)\right)\alpha^3$	19.96 ± 0.04
2	$-2 - \frac{9}{2}\alpha + \left(-\frac{67}{2} + 4\zeta(3)\right)\alpha^2 + \left(-\frac{773}{2} - \frac{\pi^4}{15} + 31\zeta(3)\right)\alpha^3$	14.80 ± 0.02
1	$-2 - 3\alpha + \left(-\frac{43}{3} + 2\zeta(3)\right)\alpha^2 + \left(-\frac{305}{3} - \frac{\pi^4}{60} + \frac{29}{3}\zeta(3)\right)\alpha^3$	9.60 ± 0.01
0	$-2 - \frac{3}{2}\alpha + \left(-\frac{19}{6} + \frac{2}{3}\zeta(3)\right)\alpha^2 + \left(-\frac{103}{12} + \frac{4}{3}\zeta(3)\right)\alpha^3$	
-1	-2	
-2	$-2 + \frac{3}{2}\alpha - \frac{29}{6}\alpha^2 + \left(\frac{94}{3} - \frac{1}{3}\zeta(3)\right)\alpha^3$	5.8 ± 1.8
-3	$-2 + 3\alpha + \left(-\frac{53}{3} + \frac{2}{3}\zeta(3)\right)\alpha^2 + \left(\frac{578}{3} + \frac{\pi^4}{60} - \frac{17}{3}\zeta(3)\right)\alpha^3$	10.50 ± 0.11
-4	$-2 + \frac{9}{2}\alpha + \left(-\frac{77}{2} + 2\zeta(3)\right)\alpha^2 + \left(\frac{2365}{4} + \frac{\pi^4}{15} - 22\zeta(3)\right)\alpha^3$	15.69 ± 0.05
-5	$-2 + 6\alpha + \left(-\frac{202}{3} + 4\zeta(3)\right)\alpha^2 + \left(\frac{4003}{3} + \frac{\pi^4}{6} - \frac{166}{3}\zeta(3)\right)\alpha^3$	20.85 ± 0.07

TABLE 8. Non-linear DSE in $D = 4$ dimensions. $\ln(\bar{\delta}(\alpha))$ is the logarithm of the shift in the renormalization point between MOM- and MS-scheme eq. (2.15). Shown are the first terms of its perturbative power series. f_{n+1}/f_n is the growth rate of the function $f(\alpha)$ in eq. (6.15).

s	$10^6 \cdot S(s)$
5	-48.879 979 612 936 267 148 575 174 247 043 686 402 701 421 680 529
4	-33.683 126 435 179 258 367 949 154 667 346 857 343 063 662 040 223
3	-16.197 057 487 106 552 084 835 982 615 789 341 267 879 644 562 145
2	-2.874 931 066 358 404 169 842 007 765 677 311 801 515 635 631 211 6
1	-0.005 037 643 852 252 104 613 165 864 641 040 152 093 341 435 216 537 2
-2	87 595.552 909 179 124 483 795 447 421 262 990 627 388 017 406 822
-3	17 853.256 793 175 269 493 347 991 077 950 813 245 133 374 820 922
-4	6637.593 110 037 931 650 951 894 178 458 603 722 595 701 766 465 0
-5	3384.186 761 682 513 227 965 148 628 942 508 807 465 013 504 317 6

TABLE 9. First 50 digits of the Stokes constant $S(s)$ for $D = 6$, see eq. (6.9).

s	$\ln(\delta(\alpha))$
5	$-\frac{8}{3} + \frac{61}{24}\alpha + \left(-\frac{80213}{7776} + \frac{7}{18}\zeta(3)\right)\alpha^2 + \left(\frac{8813575}{139968} + \frac{7\pi^4}{2592} - \frac{2563}{1296}\zeta(3)\right)\alpha^3$
4	$-\frac{8}{3} + \frac{305}{144}\alpha + \left(-\frac{331345}{46656} + \frac{5}{18}\zeta(3)\right)\alpha^2 + \left(\frac{119812205}{3359232} + \frac{\pi^4}{648} - \frac{2255}{1944}\zeta(3)\right)\alpha^3$
3	$-\frac{8}{3} + \frac{61}{36}\alpha + \left(-\frac{52325}{11664} + \frac{5}{27}\zeta(3)\right)\alpha^2 + \left(\frac{14842891}{839808} + \frac{\pi^4}{1296} - \frac{1177}{1944}\zeta(3)\right)\alpha^3$
2	$-\frac{8}{3} + \frac{61}{48}\alpha + \left(-\frac{38381}{15552} + \frac{1}{9}\zeta(3)\right)\alpha^2 + \left(\frac{3947825}{559872} + \frac{\pi^4}{3240} - \frac{341}{1296}\zeta(3)\right)\alpha^3$
1	$-\frac{8}{3} + \frac{61}{72}\alpha + \left(-\frac{24437}{23328} + \frac{1}{18}\zeta(3)\right)\alpha^2 + \left(\frac{1560359}{839808} + \frac{\pi^4}{12960} - \frac{319}{3888}\zeta(3)\right)\alpha^3$
0	$-\frac{8}{3} + \frac{61}{144}\alpha + \left(-\frac{10493}{46656} + \frac{1}{54}\zeta(3)\right)\alpha^2 + \left(\frac{518095}{3359232} - \frac{11}{972}\zeta(3)\right)\alpha^3$
-1	$-\frac{8}{3}$
-2	$-\frac{8}{3} - \frac{61}{144}\alpha - \frac{17395}{46656}\alpha^2 + \left(-\frac{114361}{209952} + \frac{11}{3888}\zeta(3)\right)\alpha^3$
-3	$-\frac{8}{3} - \frac{61}{72}\alpha + \left(\frac{31339}{23328} + \frac{1}{54}\zeta(3)\right)\alpha^2 + \left(-\frac{359005}{104976} - \frac{\pi^4}{12960} + \frac{187}{3888}\zeta(3)\right)\alpha^3$
-4	$-\frac{8}{3} - \frac{61}{48}\alpha + \left(-\frac{45283}{15552} + \frac{1}{18}\zeta(3)\right)\alpha^2 + \left(-\frac{11830593}{1119744} - \frac{\pi^4}{3240} + \frac{121}{648}\zeta(3)\right)\alpha^3$
-5	$-\frac{8}{3} - \frac{61}{36}\alpha + \left(-\frac{59227}{11664} + \frac{1}{9}\zeta(3)\right)\alpha^2 + \left(-\frac{20089615}{839808} - \frac{\pi^4}{1296} + \frac{913}{1944}\zeta(3)\right)\alpha^3$

TABLE 10. First perturbative coefficients of $\ln(\delta(\alpha))$ for $D = 6$ dimensions.

s	$S(s)$	$b^{(1)}(s)$	$b^{(2)}(s)$
5	-0.323 584 398 140 310 305 46	-33.713 129 682 396 588 961	565.374 787 298 670
4	-0.391 335 083 719 234 905 86	-28.505 508 252 042 547 410	405.630 022 359 080
3	-0.488 736 158 026 247 795 99	-23.352 717 957 250 113 407	273.573 399 332 400
2	-0.620 736 529 443 448 896 58	-18.337 005 501 361 698 274	169.862 094 180 663
1	-0.595 434 011 519 108 439 04	-13.869 604 401 089 358 619	98.052 567 522 448 0
-2	0.636 619 772 367 581 343 08	4.467 401 100 272 339 654 7	7.978 836 295 357 26
-3	0.526 186 295 467 803 784 50	9.483 113 556 160 754 788 2	40.254 589 493 216 4
-4	0.419 256 495 256 609 057 56	14.635 903 850 953 188 791	98.974 445 168 262 5
-5	0.343 587 215 470 932 442 58	19.843 525 281 307 230 343	184.621 956 597 118

TABLE 11. First digits of the Stokes constant $S(s)$ and subleading corrections of the asymptotic growth eq. (6.9) of the anomalous dimension in the toy model section 8.

s	$\alpha \ln(\delta(\alpha(A)))$
5	$-6A - \frac{2009}{3}A^2 - \frac{11563106}{45}A^3 - \frac{173306477104}{945}A^4 - \frac{1228737945883358}{6075}A^5 - \frac{46235332362117842849}{147015}A^6$
4	$-5A - \frac{1130}{3}A^2 - \frac{4316822}{45}A^3 - \frac{59632972484}{1323}A^4 - \frac{461687074578658}{14175}A^5 - \frac{34025588969113725668}{1029105}A^6$
3	$-4A - \frac{554}{3}A^2 - \frac{1263424}{45}A^3 - \frac{10282878575}{1323}A^4 - \frac{46540947260036}{14175}A^5 - \frac{398737839692532122}{205821}A^6$
2	$-3A - \frac{217}{3}A^2 - \frac{1233338}{45}A^3 - \frac{4881119933}{1323}A^4 - \frac{3528108924854}{14175}A^5 - \frac{1074400592111547046}{25727625}A^6$
1	$-2A - \frac{55}{3}A^2 - \frac{106898}{225}A^3 - \frac{135875429}{6615}A^4 - \frac{272890120256}{23625}A^5 - \frac{2770658834393158}{25727625}A^6$
0	$-A - \frac{4}{3}A^2 - \frac{146}{45}A^3 - \frac{8864}{945}A^4 - \frac{417682}{14175}A^5 - \frac{9095176}{93555}A^6$
-1	0
-2	$A + 7A^2 + 242A^3 + 17771A^4 + 2189294A^5 + 404590470A^6$
-3	$2A + 41A^2 + \frac{92518}{25}A^3 + \frac{503885698}{735}A^4 + \frac{1639676026462}{7875}A^5 + \frac{266517331818761291}{2858625}A^6$
-4	$3A + \frac{370}{3}A^2 + \frac{4782122}{225}A^3 + \frac{48904622516}{6615}A^4 + \frac{887103429351554}{212625}A^5 + \frac{88600913717695595572}{25727625}A^6$
-5	$4A + \frac{826}{3}A^2 + \frac{3478864}{45}A^3 + \frac{287007344207}{6615}A^4 + \frac{185545372999796}{4725}A^5 + \frac{5325283832756373006}{1029105}A^6$

TABLE 12. First coefficients of $\ln(\delta(\alpha))$ in the toy model section 8, up to order α^{11} . Here, $A := (\alpha\pi)^2/4$.

REFERENCES

- [1] G. 't Hooft. “Dimensional Regularization and the Renormalization Group”. In: *Nuclear Physics B* 61 (Sept. 24, 1973), pp. 455–468. ISSN: 0550-3213. DOI: 10.1016/0550-3213(73)90376-3. URL: <https://www.sciencedirect.com/science/article/pii/0550321373903763> (visited on 05/31/2021).
- [2] G. 't Hooft and M. Veltman. “Regularization and Renormalization of Gauge Fields”. In: *Nuclear Physics B* 44.1 (July 1, 1972), pp. 189–213. ISSN: 0550-3213. DOI: 10.1016/0550-3213(72)90279-9. URL: <http://www.sciencedirect.com/science/article/pii/0550321372902799> (visited on 04/24/2020).
- [3] Inês Aniceto, Gökçe Başar, and Ricardo Schiappa. “A Primer on Resurgent Transseries and Their Asymptotics”. In: *Physics Reports. A Primer on Resurgent Transseries and Their Asymptotics* 809 (May 25, 2019), pp. 1–135. ISSN: 0370-1573. DOI: 10.1016/j.physrep.2019.02.003. URL: <https://www.sciencedirect.com/science/article/pii/S0370157319300730> (visited on 09/03/2021).
- [4] E. T. Bell. “Exponential Polynomials”. In: *Annals of Mathematics* 35.2 (1934), pp. 258–277. ISSN: 0003-486X. DOI: 10.2307/1968431. JSTOR: 1968431.
- [5] Marc Bellon. “An Efficient Method for the Solution of Schwinger–Dyson Equations for Propagators”. In: *Letters in Mathematical Physics* 94.1 (Oct. 2010), pp. 77–86. ISSN: 0377-9017, 1573-0530. DOI: 10.1007/s11005-010-0415-3. arXiv: 1005.0196. URL: <http://arxiv.org/abs/1005.0196> (visited on 04/01/2021).
- [6] Marc Bellon and Fidel A. Schaposnik. “Renormalization Group Functions for the Wess–Zumino Model: Up to 200 Loops through Hopf Algebras”. In: *Nuclear Physics B* 800.3 (Sept. 2008), pp. 517–526. ISSN: 05503213. DOI: 10.1016/j.nuclphysb.2008.02.005. arXiv: 0801.0727. URL: <http://arxiv.org/abs/0801.0727> (visited on 04/28/2021).
- [7] Marc P. Bellon. “Approximate Differential Equations for Renormalization Group Functions in Models Free of Vertex Divergencies”. In: *Nuclear Physics B* 826.3 (Feb. 21, 2010), pp. 522–531. ISSN: 0550-3213. DOI: 10.1016/j.nuclphysb.2009.11.002. URL: <https://www.sciencedirect.com/science/article/pii/S0550321309005896> (visited on 04/28/2021).
- [8] C. G. Bollini and J. J. Giambiagi. “Dimensional Renormalization : The Number of Dimensions as a Regularizing Parameter”. In: *Il Nuovo Cimento B (1971-1996)* 12.1 (Nov. 1, 1972), pp. 20–26. ISSN: 1826-9877. DOI: 10.1007/BF02895558. URL: <https://doi.org/10.1007/BF02895558> (visited on 04/25/2020).
- [9] M. Borinsky, G. Dunne, and Max Meynig. “Semiclassical Trans-Series from the Perturbative Hopf-Algebraic Dyson-Schwinger Equations: ϕ^3 QFT in 6 Dimensions”. In: 2021.
- [10] Michael Borinsky. *Generating Asymptotics for Factorially Divergent Sequences*. Version 4. Oct. 8, 2018. arXiv: 1603.01236 [math-ph]. URL: <http://arxiv.org/abs/1603.01236> (visited on 02/12/2020).
- [11] Michael Borinsky and Gerald V. Dunne. “Non-Perturbative Completion of Hopf-Algebraic Dyson-Schwinger Equations”. In: *Nuclear Physics B* 957 (Aug. 1, 2020), p. 115096. ISSN: 0550-3213. DOI: 10.1016/j.nuclphysb.2020.115096. URL: <http://www.sciencedirect.com/science/article/pii/S0550321320301826> (visited on 07/05/2020).
- [12] D. J. Broadhurst and D. Kreimer. “Combinatoric Explosion of Renormalization Tamed by Hopf Algebra: 30-Loop Pade-Borel Resummation”. In: *Physics Letters B* 475.1-2 (Feb. 2000), pp. 63–70. ISSN: 03702693. DOI: 10.1016/S0370-2693(00)00051-4. arXiv: hep-th/9912093. URL: <http://arxiv.org/abs/hep-th/9912093> (visited on 03/31/2021).
- [13] D. J. Broadhurst and D. Kreimer. “Exact Solutions of Dyson-Schwinger Equations for Iterated One-Loop Integrals and Propagator-Coupling Duality”. In: *Nuclear Physics B* 600.2 (Apr.

- 2001), pp. 403–422. ISSN: 05503213. DOI: 10.1016/S0550-3213(01)00071-2. arXiv: hep-th/0012146. URL: <http://arxiv.org/abs/hep-th/0012146> (visited on 01/18/2020).
- [14] William Celmaster and Richard J. Gonsalves. “Renormalization-Prescription Dependence of the Quantum-Chromodynamic Coupling Constant”. In: *Physical Review D* 20.6 (Sept. 15, 1979), pp. 1420–1434. DOI: 10.1103/PhysRevD.20.1420. URL: <https://link.aps.org/doi/10.1103/PhysRevD.20.1420> (visited on 07/31/2019).
- [15] J. C. Collins and A. J. Macfarlane. “New Methods for the Renormalization Group”. In: *Physical Review D* 10.4 (Aug. 15, 1974), pp. 1201–1212. DOI: 10.1103/PhysRevD.10.1201. URL: <https://link.aps.org/doi/10.1103/PhysRevD.10.1201> (visited on 05/31/2021).
- [16] Louis Comtet. *Advanced Combinatorics*. Dordrecht, Holland: D. Reidel Publishing Company, 1974. ISBN: 978-94-010-2198-2.
- [17] Alain Connes and Dirk Kreimer. “Renormalization in Quantum Field Theory and the Riemann-Hilbert Problem II: The Beta-Function, Diffeomorphisms and the Renormalization Group”. In: *Communications in Mathematical Physics* 216.1 (Jan. 2001), pp. 215–241. ISSN: 0010-3616. DOI: 10.1007/PL00005547. arXiv: hep-th/0003188. URL: <http://arxiv.org/abs/hep-th/0003188> (visited on 01/21/2020).
- [18] Alain Connes and Matilde Marcolli. *Noncommutative Geometry, Quantum Fields and Motives*. Vol. 55. Colloquium Publications. Providence, Rhode Island: American Mathematical Society, Dec. 20, 2007. ISBN: 978-0-8218-4210-2 978-1-4704-3201-0. DOI: 10.1090/coll/055. URL: <http://www.ams.org/coll/055> (visited on 02/20/2019).
- [19] Julien Courtiel and Karen Yeats. “Next-to-k Leading Log Expansions by Chord Diagrams”. In: *Communications in Mathematical Physics* 377.1 (July 1, 2020), pp. 469–501. ISSN: 1432-0916. DOI: 10.1007/s00220-020-03691-7. URL: <https://doi.org/10.1007/s00220-020-03691-7> (visited on 07/05/2021).
- [20] R. Delbourgo, D. Elliott, and D. S. McAnally. “Dimensional Renormalization in Phi3 Theory: Ladders and Rainbows”. In: *Physical Review D* 55.8 (Apr. 15, 1997), pp. 5230–5233. DOI: 10.1103/PhysRevD.55.5230. URL: <https://link.aps.org/doi/10.1103/PhysRevD.55.5230> (visited on 05/26/2021).
- [21] R. Delbourgo, A. C. Kalloniatis, and G. Thompson. “Dimensional Renormalization: Ladders and Rainbows”. In: *Physical Review D* 54.8 (Oct. 15, 1996), pp. 5373–5376. DOI: 10.1103/PhysRevD.54.5373. URL: <https://link.aps.org/doi/10.1103/PhysRevD.54.5373> (visited on 05/26/2021).
- [22] F. J. Dyson. “The S Matrix in Quantum Electrodynamics”. In: *Physical Review* 75.11 (June 1, 1949), pp. 1736–1755. DOI: 10.1103/PhysRev.75.1736. URL: <https://link.aps.org/doi/10.1103/PhysRev.75.1736> (visited on 08/20/2019).
- [23] David J. Gross. “Applications of the Renormalization Group to High-Energy Physics”. In: *Methods in Field Theory, Les Houches Session 1975*. Ed. by Roger Balian and Jean Zinn-Justin. Les Houches Session 28. North Holland / World Scientific, 1981, pp. 141–250. ISBN: 978-9971-83-078-7. URL: <https://doi.org/10.1142/0004>.
- [24] Henry Kibler. “Systems of Linear Dyson–Schwinger Equations”. In: *Mathematical Physics, Analysis and Geometry* 22.3 (Aug. 29, 2019), p. 20. ISSN: 1572-9656. DOI: 10.1007/s11040-019-9320-x. URL: <https://doi.org/10.1007/s11040-019-9320-x> (visited on 07/13/2021).
- [25] Lutz Klaczynski. *Haag’s Theorem in Renormalised Quantum Field Theories*. Feb. 1, 2016. arXiv: 1602.00662 [hep-th, physics:math-ph]. URL: <http://arxiv.org/abs/1602.00662> (visited on 11/14/2018).
- [26] Dirk Kreimer. “Etude for Linear Dyson–Schwinger Equations”. In: *Tech. Rep. IHES-P-2006-23* (Mar. 28, 2006). URL: <http://preprints.ihes.fr/2006/P/P-06-23.pdf>.
- [27] Dirk Kreimer and Karen Yeats. “An Etude in Non-Linear Dyson–Schwinger Equations”. In: *Nuclear Physics B - Proceedings Supplements*. Proceedings of the 8th DESY Workshop on

- Elementary Particle Theory 160 (Oct. 1, 2006), pp. 116–121. ISSN: 0920-5632. DOI: 10.1016/j.nuclphysbps.2006.09.036. URL: <http://www.sciencedirect.com/science/article/pii/S0920563206006347> (visited on 05/04/2020).
- [28] Olaf Krüger. “Log Expansions from Combinatorial Dyson–Schwinger Equations”. In: *Letters in Mathematical Physics* 110.8 (Aug. 1, 2020), pp. 2175–2202. ISSN: 1573-0530. DOI: 10.1007/s11005-020-01288-8. URL: <https://doi.org/10.1007/s11005-020-01288-8> (visited on 10/08/2020).
- [29] Olaf Krüger and Dirk Kreimer. “Filtrations in Dyson–Schwinger Equations: Next-to-j-Leading Log Expansions Systematically”. In: *Annals of Physics* 360 (Sept. 1, 2015), pp. 293–340. ISSN: 0003-4916. DOI: 10.1016/j.aop.2015.05.013. URL: <https://www.sciencedirect.com/science/article/pii/S0003491615001979> (visited on 07/05/2021).
- [30] G. Mack and I. T. Todorov. “Conformal-Invariant Green Functions Without Ultraviolet Divergences”. In: *Physical Review D* 8.6 (Sept. 15, 1973), pp. 1764–1787. DOI: 10.1103/PhysRevD.8.1764. URL: <https://link.aps.org/doi/10.1103/PhysRevD.8.1764> (visited on 08/04/2021).
- [31] Erik Panzer. *Hopf Algebraic Renormalization of Kreimer’s Toy Model*. Feb. 16, 2012. arXiv: 1202.3552 [hep-th, physics:math-ph]. URL: <http://arxiv.org/abs/1202.3552> (visited on 06/15/2021).
- [32] Julian Schwinger. “On the Green’s Functions of Quantized Fields. II”. In: *Proceedings of the National Academy of Sciences* 37.7 (July 1, 1951), pp. 455–459. ISSN: 0027-8424, 1091-6490. DOI: 10.1073/pnas.37.7.455. pmid: 16578384. URL: <https://www.pnas.org/content/37/7/455> (visited on 09/12/2019).
- [33] N. J. A. Sloane (editor). *The On-Line Encyclopedia of Integer Sequences*. 2018. URL: <https://oeis.org> (visited on 01/20/2021).
- [34] Karen Yeats. *Growth Estimates for Dyson-Schwinger Equations*. Oct. 13, 2008. arXiv: 0810.2249 [math-ph]. URL: <http://arxiv.org/abs/0810.2249> (visited on 08/04/2021).